



Involvement of ribosomal protein L17 and Y-Box binding protein 1 in assembly of hepatitis C virus potentially via their interaction with the 3' untranslated region of the viral genome

メタデータ	言語: English 出版者: American Society for Microbiology 公開日: 2025-07-18 キーワード (Ja): キーワード (En): hepatitis C virus, particle assembly, encapsidation, genome packaging, RPL17, YBX1 作成者: Liu, Jie メールアドレス: 所属: 浜松医科大学
URL	http://hdl.handle.net/10271/0002000461

This work is licensed under a Creative Commons Attribution 4.0 International License.



Editor's Pick | Virology | Full-Length Text

Involvement of ribosomal protein L17 and Y-box binding protein 1 in the assembly of hepatitis C virus potentially *via* their interaction with the 3' untranslated region of the viral genome

Jie Liu,¹ Masahiko Ito,¹ Liang Liu,¹ Kenji Nakashima,¹ Shinya Satoh,¹ Alu Konno,¹ Tetsuro Suzuki¹**AUTHOR AFFILIATION** See affiliation list on p. 24.

ABSTRACT The 3' untranslated region (3'UTR) of the hepatitis C virus (HCV) RNA genome, which contains a highly conserved 3' region named the 3'X-tail, plays an essential role in RNA replication and promotes viral IRES-dependent translation. Although our previous work has found a cis-acting element for genome encapsidation within 3'X, there is limited information on the involvement of the 3'UTR in particle formation. In this study, proteomic analyses identified host cell proteins that bind to the 3'UTR containing the 3'X region but not to the sequence lacking the 3'X. Further characterization showed that RNA-binding proteins, ribosomal protein L17 (RPL17), and Y-box binding protein 1 (YBX1) facilitate the efficient production of infectious HCV particles in the virus infection cells. Using small interfering RNA (siRNA)-mediated gene silencing in four assays that distinguish between the various stages of the HCV life cycle, RPL17 and YBX1 were found to be most important for particle assembly in the trans-packaging assay with replication-defective subgenomic RNA. *In vitro* assays showed that RPL17 and YBX1 bind to the 3'UTR RNA and deletion of the 3'X region attenuates their interaction. Knockdown of RPL17 or YBX1 resulted in reducing the amount of HCV RNA co-precipitating with the viral Core protein by RNA immunoprecipitation and increasing the relative distance in space between Core and double-stranded RNA by confocal imaging, suggesting that RPL17 and YBX1 potentially affect HCV RNA-Core interaction, leading to efficient nucleocapsid assembly. These host factors provide new clues to understanding the molecular mechanisms that regulate HCV particle formation.

IMPORTANCE Although basic research on the HCV life cycle has progressed significantly over the past two decades, our understanding of the molecular mechanisms that regulate the process of particle formation, in particular encapsidation of the genome or nucleocapsid assembly, has been limited. We present here, for the first time, that two RNA-binding proteins, RPL17 and YBX1, bind to the 3'X in the 3'UTR of the HCV genome, which potentially acts as a packaging signal, and facilitates the viral particle assembly. Our study revealed that RPL17 and YBX1 exert a positive effect on the interaction between HCV RNA and Core protein, suggesting that the presence of both host factors modulate an RNA structure or conformation suitable for packaging the viral genome. These findings help us to elucidate not only the regulatory mechanism of the particle assembly of HCV but also the function of host RNA-binding proteins during viral infection.

KEYWORDS hepatitis C virus, particle assembly, encapsidation, genome packaging, RPL17, YBX1

Hepatitis C virus (HCV) infection is the major cause of chronic hepatitis, hepatic cirrhosis, and hepatocellular carcinoma. The World Health Organization (WHO)

Editor J.-H. James Ou, University of Southern California, Los Angeles, California, USA

Address correspondence to Tetsuro Suzuki, tesuzuki@hama-med.ac.jp.

The authors declare no conflict of interest.

See the funding table on p. 24.

Received 19 March 2024

Accepted 27 May 2024

Copyright © 2024 American Society for Microbiology. All Rights Reserved.

estimates that 58 million people worldwide are currently persistently infected and approximately 1.5 million new infections occur annually (<https://www.who.int/news-room/fact-sheets/detail/hepatitis-c>). The genome of HCV is a positive-sense, single-stranded RNA with highly structured elements, approximately 9.6 kb in length. This genomic RNA contains one open reading frame (ORF) encoding a large precursor polyprotein, which is co- and post-translationally processed into 10 viral proteins: the structural proteins Core, E1, E2, and p7 and the non-structural proteins NS2, NS3, NS4A, NS4B, NS5A, and NS5B. The 5′ untranslated region (5′UTR) and 3′ untranslated region (3′UTR) exist at the 5′ and 3′ ends of the genome, respectively. Both UTRs are highly structured and well conserved among HCV genotypes and strains. Most of the 5′UTR is occupied by the internal ribosomal entry site (IRES), which is involved in the initiation of viral protein synthesis and is essential for genome replication. The 3′UTR is between 200 and 235 nt in length and contains a short variable region, a poly(U/UC) stretch of approximately 90 nt in length, and a 98 nt X-tail region (3′X) which is an almost absolutely conserved sequence. The 3′X region is essential for viral replication and contributes to the translation efficiency of viral polyproteins by modulating the exposure of a nucleotide segment involved in a distal base-pairing interaction with an upstream 5BSL3.2 domain, which is a part of the essential *cis*-acting replication element located in the NS5B coding sequence (1). The 3′X region and the IRES of the 5′UTR establish a distal RNA-RNA contact network and contribute to viral replication (2).

The formation of infectious viral particles requires coordinated packaging of the viral genome into nucleocapsids. Among the various stages of the HCV life cycle, the molecular mechanisms of encapsidation of the genomic RNA are not fully understood. The matured form of Core, the viral capsid protein (p21), is composed of two functional domains: the first is a highly basic, hydrophilic N-terminal domain that is involved in interaction with HCV genomic RNA and oligomerization of the capsid around the genome; the C-terminal hydrophobic domain is responsible for the association of Core with the membrane proteins and lipid droplets (LDs). This domain is not present in the capsid proteins of the most of other members of *Flaviviridae* family. Cytosolic LDs have been proposed to act as a platform for the assembly of HCV particles (3–5). NS5A, a multifunctional RNA-binding phosphoprotein and a component of the viral replication complex, is also known to traffic to LDs where it colocalizes with Core and this colocalization appears to be required for the particle assembly (6–8). The synthesized viral genomes might be released, together with NS5A, from the replication complex and be recruited to the surface of LDs, enabling its interaction with Core. It thus appears that NS5A potentially coordinates the steps from the genome replication to the virion assembly (9, 10).

In general, for RNA viruses, the packaging of viral RNA genomes into nucleocapsids requires a distinct RNA structure, for example, near the 5′ end of the RNA genome, as has been shown for retroviruses and alphaviruses (11–13). An early study using a series of mutants within the 5′UTR of the HCV genome has shown that the 5′UTR is unlikely to contain the *cis*-acting RNA structures required for viral encapsidation (14). A recent study has shown that the energetically favored alternative conformation of stem-loop II (SLII^{alt}) within the 5′UTR possibly promotes virion assembly, whereas spontaneous or Argonaute/miR-122-mediated conversion to the SLII conformation is involved in viral RNA translation (15). By contrast, we have identified 3′X region within the 3′UTR as a *cis*-acting element which is important for HCV genome packaging (16, 17). In trans-packaging systems with both replicative- and replication-defective HCV subgenomes, deletion of the 3′UTR in the subgenomes reduced production of trans-complemented HCV particles to background levels, whereas deletion of the 5′UTR resulted in only a small reduction. Furthermore, the modified trans-packaging assay introducing a reporter gene cassette showed that, while the 5′UTR potentially supports the packaging of foreign RNA, it does so much less efficiently than the 3′UTR.

In this study, to better understand the molecular mechanisms that regulate the encapsidation of the HCV genome, we searched for host-derived factors that bind to

the 3'UTR sequence containing the 3'X region but not to the sequence lacking the 3'X, followed by knockdown analysis in HCV-infected cells. We identify the 3'X-binding proteins, ribosomal protein L17 (RPL17) and Y-box binding protein 1 (YBX1), involved in the assembly of HCV particles.

RESULTS

Identification of host factors binding to the 3'X region of HCV 3'UTR in the viral genome

To identify novel host factors involved in HCV particle formation, first, we searched for cellular proteins with the ability to bind to the 3'X region in the 3'UTR, a cis-element that is important for HCV genome packaging. *In vitro* transcribed HCV subgenomic (SGR WT) RNA derived from JFH-1 isolate and its 3'X region-deleted (SGR Δ3'X) RNA were electroporated into the viral Core-NS2 stable expressing cells, followed by recovering HCV RNA-protein complexes from the cell lysates using streptavidin-coated beads and biotinylated HCV RNA complementary DNA probes (Fig. S1). Among the proteins identified by LC-MS/MS analysis, representative proteins, YBX1, RPL17, ALDH1A3, GCDH, SERBP1, NIM1K, and ZNF132 that did not show binding to the SGR Δ3'X RNA are listed in the upper part of Table 1. It was confirmed that our screening system also found proteins that showed binding to SGR Δ3'X RNA, such as HNRNPM, DROSHA, and TRMT11 in the lower part of the list.

Based on the results of the proteomic screening, RPL17 and YBX1, which showed high binding to HCV SGR RNA, relatively high sequence coverage in MS analysis, and no binding to SGR Δ3'X RNA, were next investigated for their involvement in the HCV life cycle.

Reduction of infectious HCV production by knockdown of RPL17 or YBX1

To determine whether RPL17 and YBX1 are involved in the production of infectious HCV in Huh7.5.1 cells highly susceptible to HCV infection, the cells with RPL17- or YBX1 knockdown were infected with HCV (J6/JFH-1), and 3 days later the cell culture supernatants were inoculated into naive Huh7.5.1 cells to determine the infectious titers. Accumulating evidence shows that the very low-density-lipoprotein component apolipoprotein E (ApoE) plays a major role in the formation of infectious HCV particles, presumably *via* contributing to the maturation and secretion of the viral particles (18–20). Thus, ApoE knockdown was used as a positive control for inhibition of HCV particle formation. Under knockdown conditions where the mRNA expression of RPL17 and YBX1 was reduced to below 20% (Fig. 1A), the infectious titers of HCV particles in

TABLE 1 Host factors binding to the 3'X region of HCV 3'UTR identified by LC-MS/MS^a

Gene	Accession ^b	Coverage ^c [%]	Abundance ^d		Description ^e
			SGR	SGR Δ3'X	
YBX1	P67809	12	71436	0	Y-Box binding protein 1
RPL17	P18621	7	69725	0	Ribosomal protein L17
ALDH1A3	P47895	5	1349351	0	Aldehyde dehydrogenase enzyme
GCDH	Q92947	5	46911456	0	Acyl-CoA dehydrogenase enzyme
SERBP1	Q8NC51	4	19370	0	SERPINE1 mRNA binding protein
NIM1K	Q8IY84	4	23505	0	Serine/threonine protein kinase
ZNF132	P52740	4	582116	0	Zinc finger protein 132
HNRNPM	P52272	1	101370	75981	Heterogeneous nuclear ribonucleoprotein M
DROSHA	Q9NRR4	1	186880	96412	Drosha ribonuclease III
TRMT11	Q7Z4G4	1	221993	100300	TRNA Methyltransferase 11 Homolog

^aAn outline of the preparation of cellular proteins that bind to HCV subgenomic replicon (SGR) RNA or 3'X region-deleted subgenomic replicon (SGR Δ3'X) RNA is indicated in Fig. S1.

^bAccession no. in UniProt databases.

^cPercentage of the region within the protein covered by identified peptides.

^dAbundance of the sum of the identified peptides.

^eGene description from the database of human genes, GeneCards.

the supernatant of RPL17- or YBX1-knockdown cells were reduced to less than 20% compared to control siRNA-transfected cells. The reduction rates of infectious titer were greater than that in case of ApoE-knockdown, which was performed as a control for inhibition of HCV particle production (Fig. 1B). While intracellular HCV RNA level in RPL17 knockdown cells was comparable to control cells, the viral RNA level was reduced by approximately 50% in YBX1 knockdown cells (Fig. 1C), suggesting that YBX1 may have some role in RNA replication of HCV. Nuclease-resistant fractions of the supernatants from the knockdown cells were prepared and HCV RNAs were measured therein, which

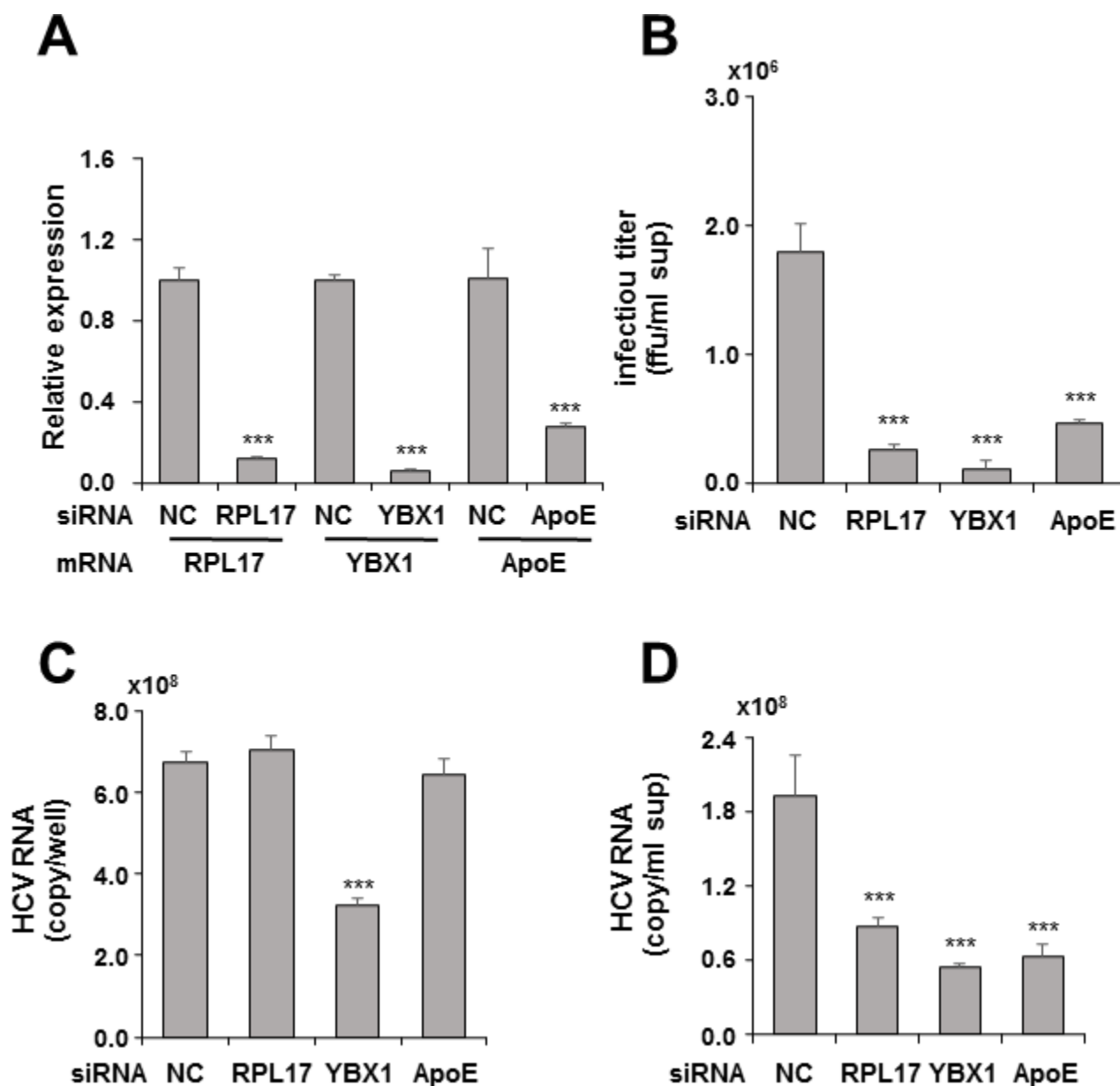


FIG 1 Virus production in Huh7.5.1 cells infected with HCV J6/JFH-1 was reduced by knocking down RPL17 and YBX1. Huh7.5.1 cells were transfected with siRNA against RPL17 or YBX1 or negative control (NC) siRNA and infected with HCV J6/JFH-1 (MOI = 0.2). Cell lysates and culture supernatants were harvested at 3 days post-infection (dpi). (A) mRNA expression levels of RPL17, YBX1, and ApoE in siRNA-treated cells were determined by qRT-PCR. (B) To determine the focus-forming unit, the culture supernatants collected were inoculated to naive Huh7.5.1 cells, followed by immunostaining with anti-Core antibody at 3 dpi. HCV RNA copies in the siRNA-treated cells collected as above (C) and copies of particle-associated HCV RNA prepared from their culture supernatants (D) were quantified by qRT-PCR. Results are presented as means \pm SD ($n = 3$). Statistical analysis was conducted by ANOVA with post hoc Tukey's test for pairwise group comparisons. *** $P < 0.001$.

showed a significant reduction in HCV levels in that from RPL17- or YBX1 knockdown cells (Fig. 1D), similar to the results in Fig. 1B.

A similar analysis was performed using persistently infected Huh-7 cells (HC-PI cells), which continuously produce HCV JFH-1 at a moderately low level. When culture supernatants from RPL17- or YBX1-knockdown HC-PI cells with siRNAs-transfection were inoculated into naive Huh7.5.1 cells and intracellular HCV RNAs were measured, HCV RNA levels were reduced by more than 60% and 80% in the case of RPL17- and YBX1 knockdown, respectively, compared to control (Fig. 2A). In knockdown HC-PI cells, intracellular HCV RNAs were comparable to control in RPL17 knockdown and approximately 30% lower in YBX1 knockdown (Fig. 2B), suggesting that YBX1, but not RPL17, may be involved to some extent in the viral RNA replication. The amounts of HCV RNA in the nuclease-resistant fraction of the culture supernatant of these cells were reduced by more than 70% with RPL17 knockdown and 80% with YBX1 knockdown (Fig. 2C). The knockdown efficiencies with each siRNA and protein are as shown in Fig. 2D and E.

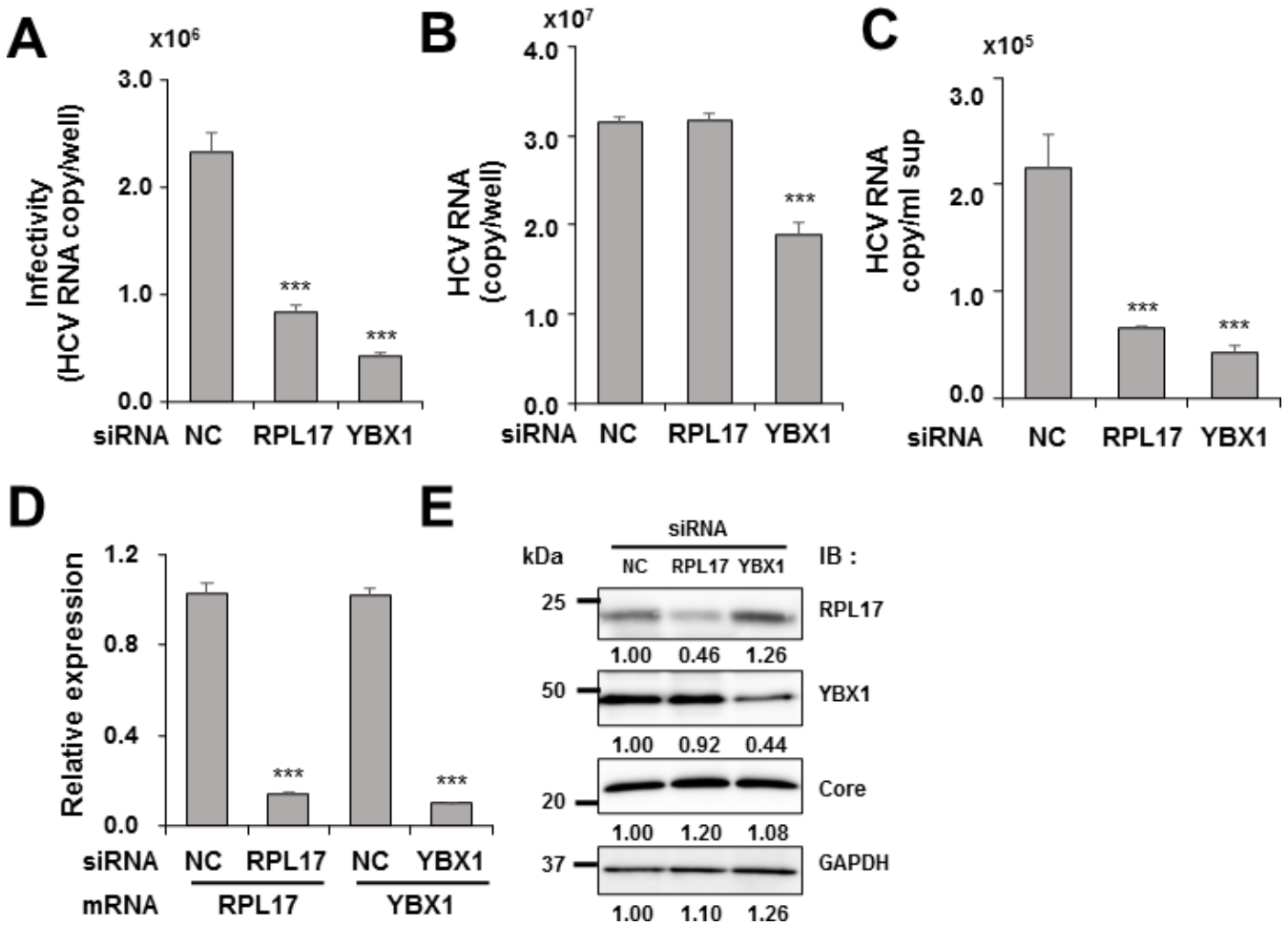


FIG 2 Reduction of HCV production by knockdown of RPL17 and YBX1 in HuH-7 cells constitutively infected with HCV JFH-1 (HC-PI cells). HC-PI cells were transfected with siRNA against RPL17 or YBX1 or negative control (NC) siRNA. After culturing for 3 days, the culture supernatants collected were inoculated to naive Huh7.5.1 cells, followed by measurement of HCV RNA copies at 3 dpi to determine the viral transduction (A). HCV RNA copies in the siRNA-treated cells (B) and copies of particle-associated HCV RNA prepared from their culture supernatants (C) were determined. (D) mRNA expression levels of RPL17 and YBX1 in siRNA-treated HC-PI cells were determined by qRT-PCR. Results are presented as means \pm SD ($n = 4$). (E) Protein expression of RPL17, YBX1, HCV Core, and GAPDH in siRNA-treated HC-PI cells were examined by immunoblotting, and protein levels were quantified by ImageJ. The intensity of each protein band for siRNA NC-transfected cells was set as 1, and the relative values were determined for siRPL17- or siYBX1-transfected cells. Statistical analysis was conducted by ANOVA with post hoc Tukey's test for pairwise group comparisons. *** $P < 0.001$.

To confirm that this inhibition of HCV production by gene knockdown was not due to off-target effects of the siRNAs, rescue experiments were performed using RPL17 or YBX1 expression vectors. Cells with RPL17 or YBX1 knockdown were infected with HCV after transfection with siRNA-resistant RPL17- or YBX1 expression plasmids. HCV production was suppressed by more than 80% by RPL17- or YBX1 knockdown, and HCV production was significantly restored by introducing siRNA-resistant RPL17- or YBX1 expression vectors into the knockdown cells (Fig. 3A). The amount of HCV RNA in the nuclease-resistant fraction of the culture supernatant also showed similar changes with each knockdown and expression vector introduction (Fig. 3B). Protein expression of RPL17 and YBX1 in cells of the rescue experiments is shown in Fig. 3C.

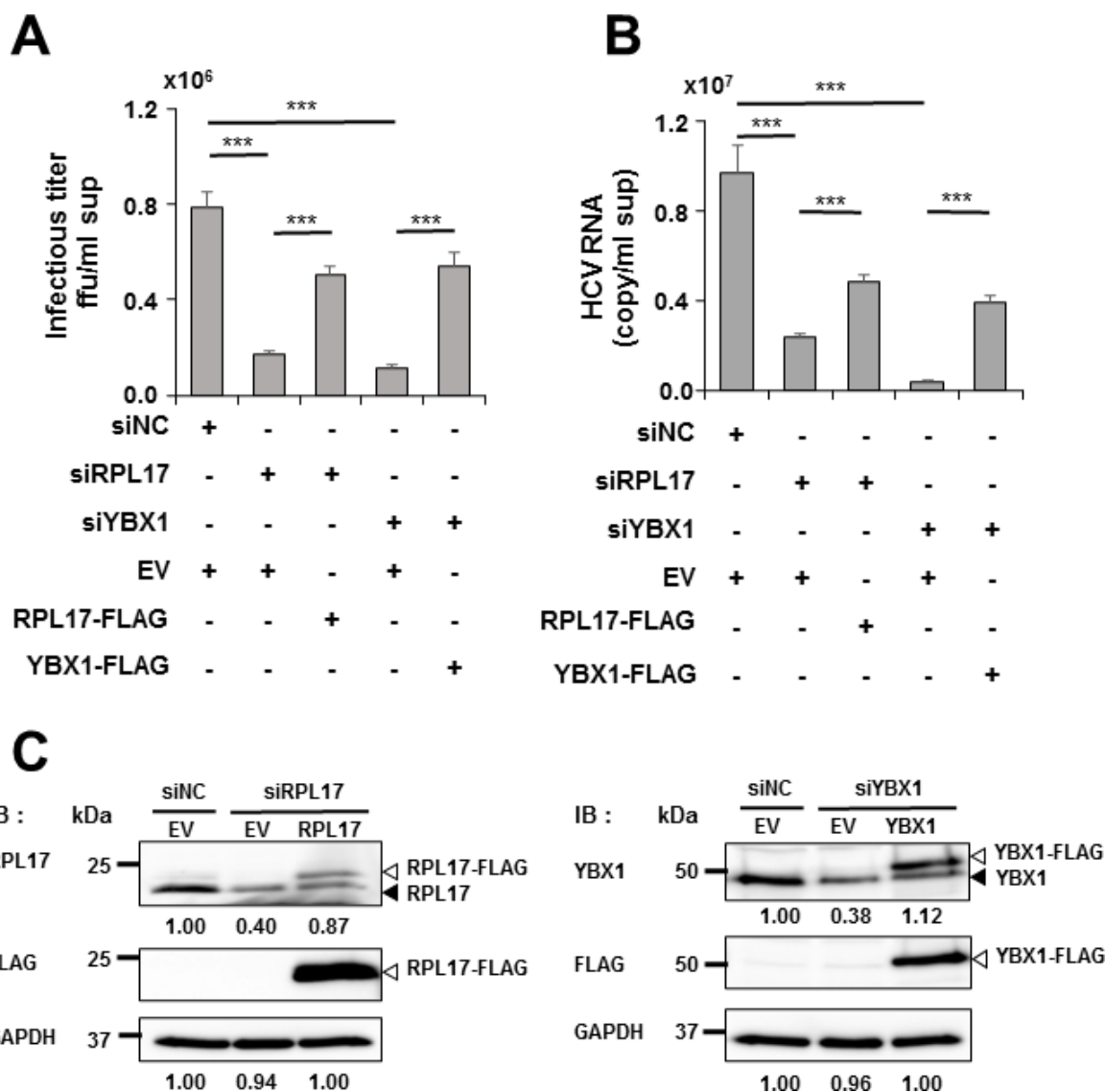


FIG 3 Reduced HCV production was rescued by ectopic expression of RPL17 and YBX1. At 1 day post-transfection with siRNA against RPL17 or YBX1 or negative control (NC) siRNA as well as the expression plasmid for FLAG-tagged RPL17 or YBX1 or an empty vector (EV), Huh7.5.1 cells were infected with HCV J6/JFH-1 and further cultured for 2 days. (A) To determine the focus-forming unit, the culture supernatants collected were inoculated to naive Huh7.5.1 cells, followed by immunostaining with anti-Core antibody. (B) Particle-associated HCV samples were prepared from the culture supernatants and the viral RNA copies were determined by qRT-PCR. Results are presented as means \pm SD ($n = 3$). (C) Protein expression of RPL17, YBX1, and GAPDH in siRNA-treated cells was examined by immunoblotting, and protein levels were quantified by ImageJ. The intensity of each protein band for plasmid EV and siRNA NC-transfected cells was set as 1, and the relative values were determined for siRPL17- or siYBX1-transfected cells. Statistical analysis was conducted by ANOVA with post hoc Tukey's test for pairwise group comparisons. *** $P < 0.001$.

Thus, these results demonstrate that RPL17 and YBX1, identified as host factors with the ability to bind to the 3'X region within the 3'UTR of the HCV genome, contribute to the production of infectious HCV.

We next investigated whether particle production is affected when RPL17 and YBX1 are knocked down simultaneously. siRNAs against RPL17 or YBX1 were introduced simultaneously or separately into HC-PI cells and cultured for 3 days. Intracellular HCV RNA levels in Huh7.5.1 cells inoculated with culture supernatant from knockdown cells were reduced by 60%–70% by knockdown of RPL17 or YBX1 alone, while double knockdown had the same level of inhibition of HCV production (Fig. 4A). No significantly greater reduction in particle production was observed with double knockdown compared to single factor knockdown. Cell viability analysis showed that double knockdown of RPL17 and YBX1 affects the cellular environment (Fig. 4B), which may be difficult to assess accurately, at least under experimental conditions.

Binding model of RPL17 and YBX1 to the 3'UTR of HCV RNA

To elucidate critical RNA sequence and secondary structure(s) within the HCV genomic 3'UTR, which is critical for binding of RPL17 and YBX1 to the viral RNA, various mutant RNAs were synthesized and their binding abilities to recombinant RPL17 and YBX1 were analyzed *in vitro* by AlphaScreen (Fig. 5). As expected, both RPL17 and YBX1 showed high levels of binding to SGR RNA ("SGR" in Fig. 5A), and their RNA binding was significantly reduced when the 3'X region was deleted from SGR sequence (SGR Δ 3'X). RPL17 and YBX1 exhibited high levels of binding to the 98 base RNA with only the 3'X (3'X); no specific binding to RNA was observed when GFP was used instead of RPL17 and YBX1 (Fig. 5A).

Although there are three stem-loop structures in the 3'X region of the viral 3'UTR, it has already been shown that the loss of SLIII region has minimal influence on HCV

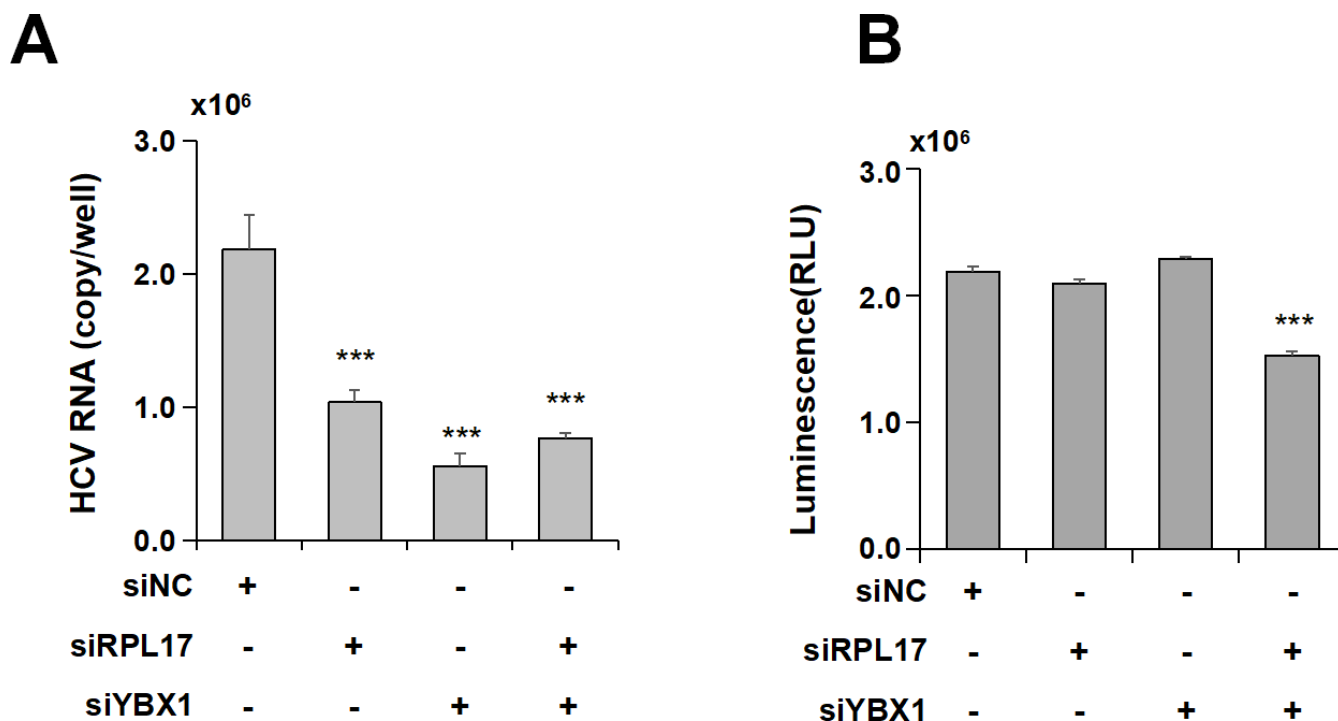


FIG 4 Effect of double-knockdown of RPL17 and YBX1 on HCV production. Huh-7 cells constitutively infected with HCV JFH-1 (HC-PI cells) were transfected with siRNA against RPL17 and/or YBX1 or negative control (NC) siRNA and cultured for 3 days. The culture supernatants collected were inoculated to naive Huh7.5.1 cells, followed by measurement of HCV RNA copies at 3 dpi to determine the viral infectivity (A). Cell viability was analyzed by using Cell Titer-Glo luminescent (B). Results are presented as means \pm SD ($n = 4$). Statistical analysis was conducted by ANOVA with post hoc Tukey's test for pairwise group comparisons. $***P < 0.001$.

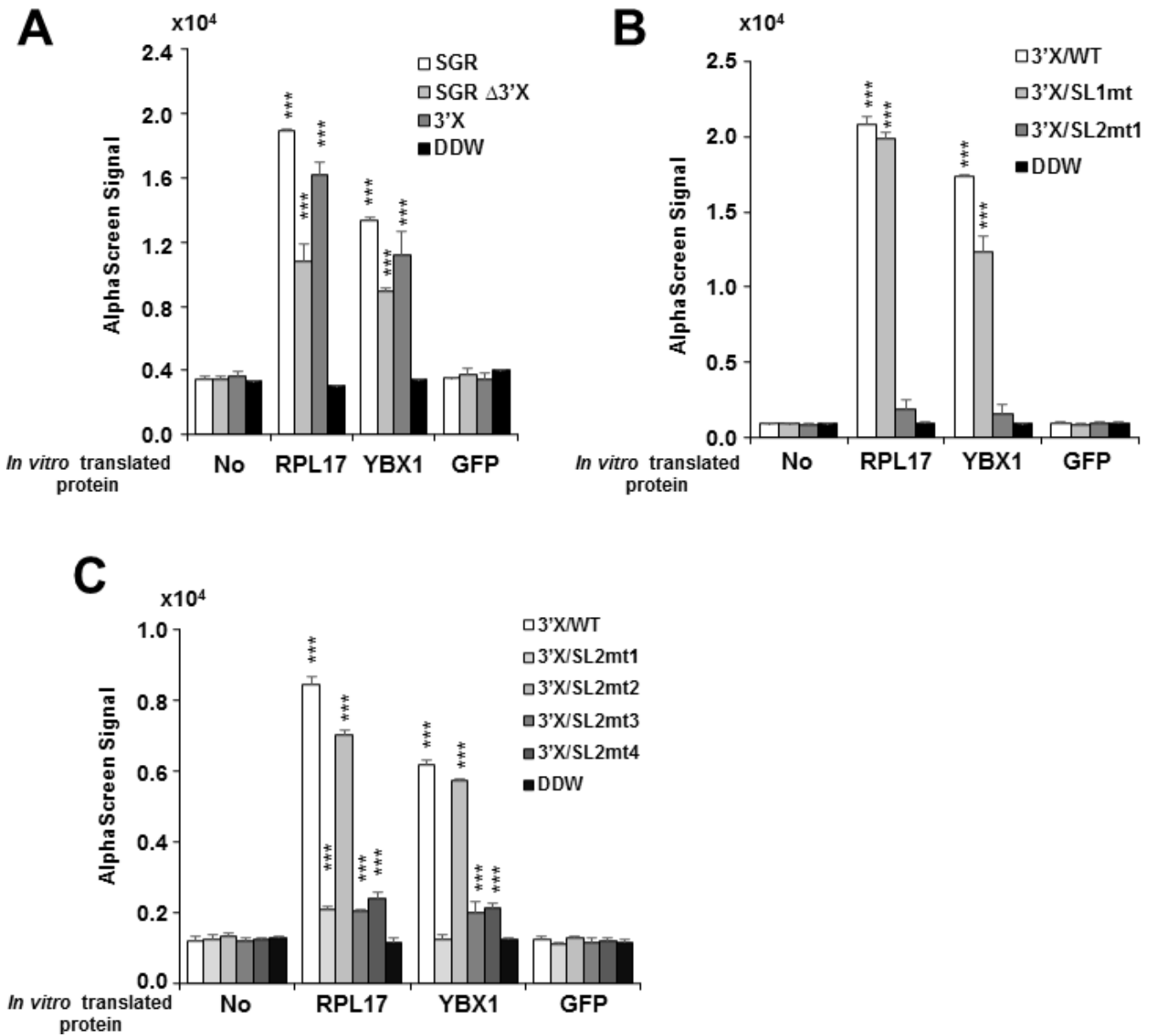


FIG 5 *In vitro* binding of RPL17 and YBX1 with HCV RNAs. (A) Interactions between *in vitro* transcribed HCV RNA: SGR, SGR without 3'X region or 3'X region and *in vitro* translated RPL17, YBX1, and GFP were examined by AlphaScreen. DDW: without HCV RNA. (B) Interactions between *in vitro* transcribed HCV RNA: 3'X/WT, 3'X/SL1mt, and 3'X/SL2mt1 and *in vitro* translated RPL17, YBX1, and GFP was examined by AlphaScreen. DDW: without HCV RNA. (C) Interactions between *in vitro* transcribed HCV RNA: wild-type (WT) or mutated sequences of 3'X region (see Fig. S3) and *in vitro* translated RPL17, YBX1, and GFP were examined by AlphaScreen. DDW: without HCV RNA. Results are presented as means ± SD (*n* = 3). Statistical analysis was conducted by ANOVA with post hoc Tukey's test for pairwise group comparisons. (A) For RPL17, the statistical significance is represented by comparing RPL17-DDW with RPL17-SGR, RPL17-SGR Δ3'X, or RPL17-3'X. For YBX1: the statistical significance is represented by comparing YBX1-DDW with YBX1-SGR, YBX1-SGR Δ3'X, or YBX1-3'X. (B) For RPL17: the statistical significance is represented by comparing RPL17-DDW with RPL17-3'X/WT, RPL17-3'X/SL1mt, and RPL17-3'X/SL2mt1. For YBX1: the statistical significance is represented by comparing YBX1-DDW with YBX1-3'X/WT, YBX1-3'X/SL1mt, and YBX1-3'X/SL2mt1. (C) For RPL17: the statistical significance is represented by comparing RPL17-DDW with RPL17-3'X/WT or RPL17-3'X/SL2mt1-mt4. For YBX1: the statistical significance is represented by comparing YBX1-DDW with YBX1-3'X/WT or YBX1-3'X/SL2mt1-mt4. ****P* < 0.001.

particle production (16). We synthesized two substitution mutants that changed the secondary structures of SLI, which is closest to the 3' ends, and SLII, which is on the 5' sides of SLI, respectively (Fig. S3A and S3B), and assessed their binding abilities to RPL17 and YBX1. The results showed that the SLI mutant (3'X/SL1mt) did not significantly

change the binding ability to both host factors, while the SLII mutant (3'X/SL2mt1) markedly decreased the binding ability (Fig. 5B). Furthermore, mutant RNAs in the stem and loop regions of SLII were designed (Fig. S3A and S3B) and examined for the binding to host factors. A mutant RNA that significantly altered the loop structure (3'X/SL2mt2) maintained its binding ability to RPL17 and YBX1, whereas mutations that closed the loop structure (3'X/SL2mt3) or substituted four bases in the same region while retaining the loop structure (3'X/SL2mt4) resulted in a marked reduction in the binding ability (Fig. 5C). Quality and the size of *in vitro* synthesized HCV RNAs used in this binding assay are confirmed (Fig. S2, S3C, and D). These results suggest that SLII in the 3'UTR, especially the loop region, plays an important role in the binding of RPL17 and YBX1 to the HCV genome.

YBX1 protein is composed of three structural domains: an N-terminal domain, a cold shock domain (CSD), and a C-terminal tail domain (Fig. 6A). The CSD is highly conserved among members of the Y-box protein family and contains an RNA-binding motif (21). As expected, immunoprecipitation RT-qPCR analysis showed that mutant YBX1 lacking the CSD region (Δ CSD)(Fig. 6B) lost its binding ability to HCV RNA (Fig. 6C). On the other hand, no functional region has been reported for RPL17. Thus, the RPL17 protein was divided into approximately three equal regions basically based essentially on secondary structural features inferred from the amino acid sequence (Fig. 6A; Fig. S3E). Each deletion mutant and full-length RPL17 were synthesized *in vitro* (Fig. 6B) and analyzed for binding to HCV RNA as in the case of YBX1. The 63-residue region on the N-terminal side of RPL17 was shown not to be involved in RNA binding while deletion of the M or C region clearly reduced RNA-binding ability (Fig. 6D).

Effects of RPL17- or YBX1 knockdown on HCV entry into cells, IRES-dependent translation, RNA replication, and particle assembly

Next, to determine the molecular mechanisms by which RPL17 and YBX1 are involved in the production of infectious viruses, the effects of gene knockdown on each step of the HCV life cycle were investigated. The process of HCV entry into cells was analyzed using the HCV pseudoparticle (HCVpp) infection assay (Fig. 7A) and the IRES-dependent translation was assessed using a dicistronic reporter assay (Fig. 7B). Neither RPL17 nor YBX1 knockdown had any effect on activity in HCVpp infection and IRES-dependent translation (Fig. 7A and B). CD81 siRNA in the HCVpp assay and LA peptide-WT but not -Y23Q mutant in the IRES reporter assay, used as controls, showed inhibition of HCV entry and HCV translation activity, respectively. The effects of RPL17 and YBX1 on HCV RNA replication were evaluated using two types of cells persistently replicating subgenomic HCV replicons derived from genotypes 2a (SGR-GT2a) and 1b (SGR-GT1b). RPL17 knockdown increased HCV RNA levels by 20%–30% in SGR-GT2a and -GT1b cells. On the other hand, in the case of YBX1 knockdown, a ~20% decrease in HCV RNA levels was observed in both SGR cells (Fig. 7C). As in the case of HCV infection, it is suggested that YBX1 has a moderate effect on the viral RNA replication. Western blot analyses of HCV proteins expressed in both SGR cells showed that the expression levels of NS5A and NS3 proteins were not significantly altered by either RPL17 or YBX1 knockdown (Fig. 7C and D). It is noted that RPL17 and YBX1 mRNA expression was reduced to less than 30% by gene knockdown in all three experiments: HCVpp infection, IRES reporter, and SGR assays (Fig. 7E).

To further analyze the role of RPL17 and YBX1 in the process of particle assembly, we performed a knockdown of both factors in a particle production system independent of RNA replication (*trans* packaging assay). HCV Core-NS2 was co-expressed either with RNA from the HCV subgenomic replicon containing a point mutation within the active center of the NS5B polymerase (SGR-GND) or its X region deletion in the 3'UTR (GND-3'Xdel) in Huh7.5.1 cells to produce HCV particles (producer cells). After the knockdown of RPL17 or YBX1 in the producer cells, their culture supernatants were collected and inoculated into naive cells. HCV RNA levels in the transducer cells were used as an indicator of particle production. Knockdown of RPL17 or YBX1 in cells co-expressing SGR-GND RNA

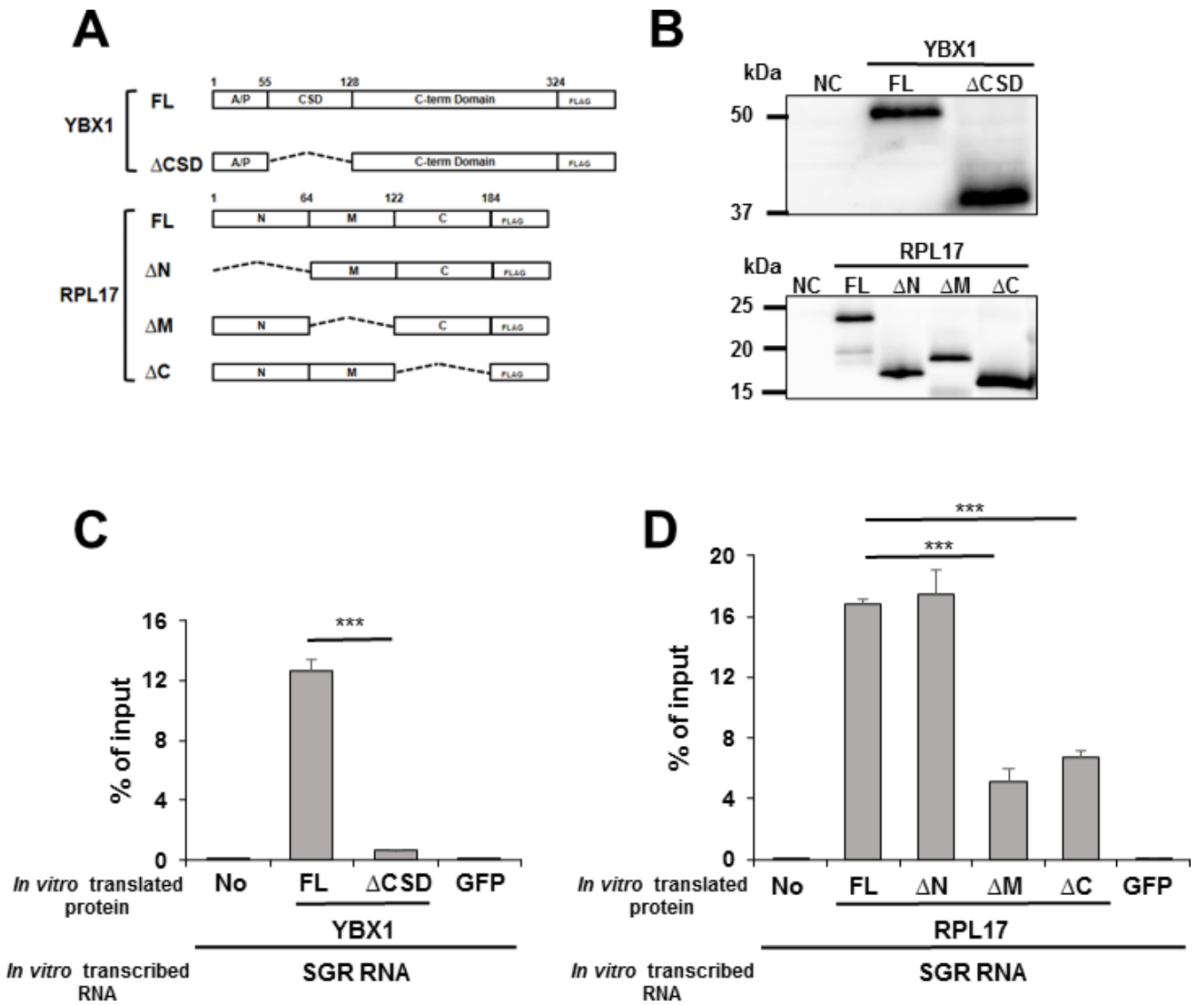


FIG 6 *In vitro* binding of HCV RNAs with RPL17, YBX1, and their mutants. (A) Schematic illustration of full-length (FL) and truncated versions of RPL17 and YBX1 used for panels (C) and (D). All synthetic proteins have a FLAG tag attached to the C-terminus. (B) Full-length (FL) and truncated forms of YBX1 and RPL17 synthesized *in vitro* were examined by immunoblotting. (C) *In vitro* RIP assay using HCV SGR RNA with YBX1 and GFP. Y axis indicates the ratio of immunoprecipitated HCV RNA copies to the input RNA copies. (D) *In vitro* RIP assay using the SGR RNA with RPL17 and GFP. Results are presented as means \pm SD ($n = 3$). Statistical analysis was conducted by ANOVA with post hoc Tukey's test for pairwise group comparisons. (C) The statistical significance is represented by comparing YBX1(FL)-SGR with YBX1(Δ CSD)-SGR. (D) The statistical significance is represented by comparing RPL17(FL)-SGR with RPL17(Δ N-C)-SGR. **** $P < 0.001$.

and Core-NS2 reduced particle production to approximately 40% or less, as indicated by measurement of the viral RNA in the transducer cells (Fig. 8A, sample group #1 versus #3, 5). Comparing the non-replicating replicons with and without the 3'X sequence, we found that particle production with GND-3'Xdel was less efficient than with SGR-GND, down to less than 40% efficiency in particle production, as previously reported (16) (Fig. 8A, sample group #1 versus #2). Knockdown of RPL17 or YBX1 in the producer cells expressing GND-3'Xdel RNA together with Core-NS2 resulted in further reduction of particle production (Fig. 8A, sample group #2 versus #4, 6). HCV RNA levels in the nuclease-resistant fractions of the culture supernatants of the producer cells showed a similar trend as the viral RNAs in the transducer cells, that is, a significant reduction by loss of the 3'X sequence or knockdown of RPL17 and YBX1 (Fig. 8B). We confirmed that knockdown of RPL17 or YBX1 significantly reduced its expression of both factors (Fig. 8C)

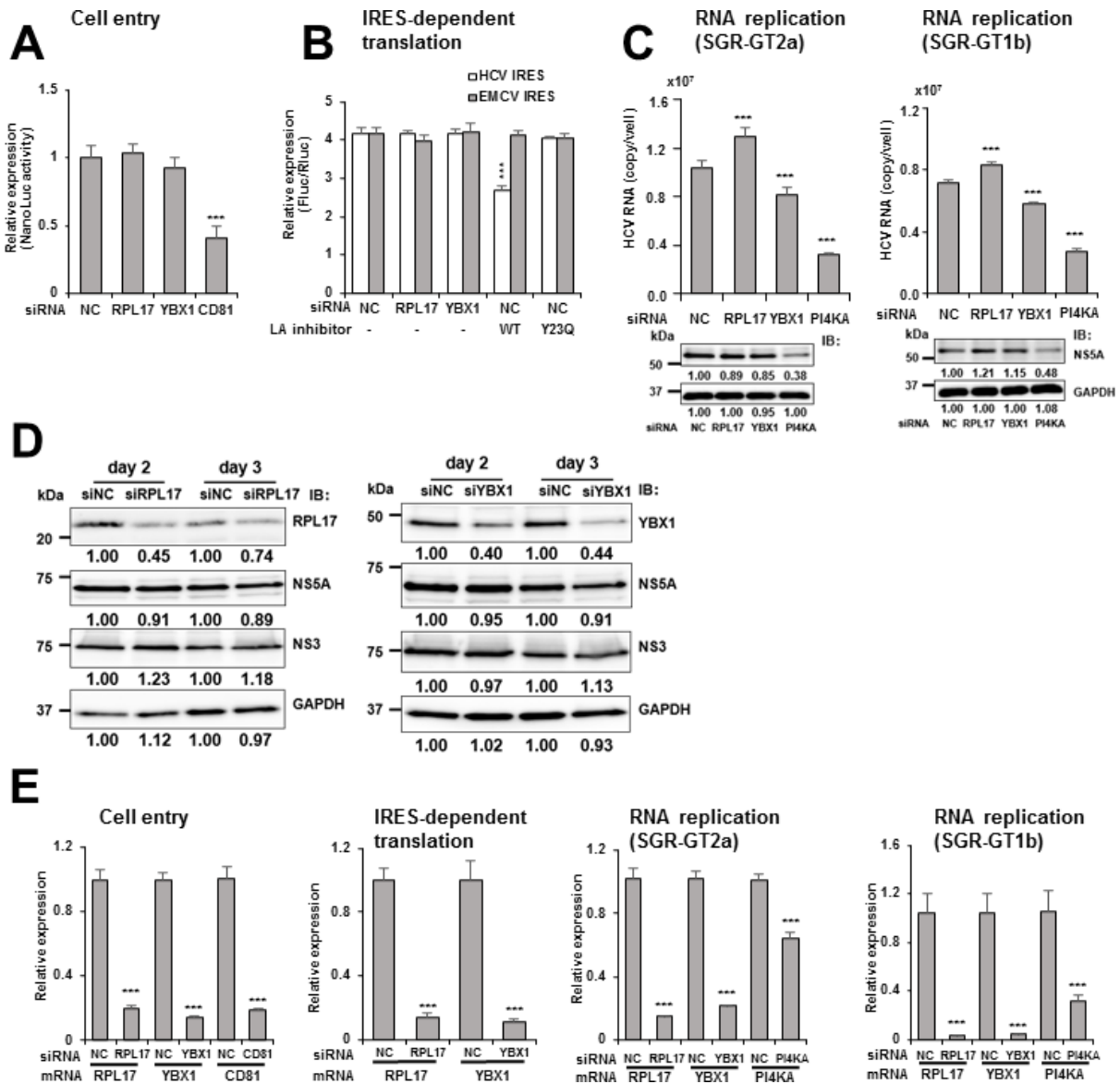


FIG 7 Effect of knocking down of RPL17 and YBX1 on cell entry, IRES-dependent translation and RNA replication of HCV. (A) Huh7.5.1 cells were transfected with siRNA and infected with HCVpp. After incubation for 2 days, NanoLuc activity in cell lysate was measured ($n = 3$). (B) *In vitro* transcribed RNAs of RLuc-HCV IRES-FLuc-3' UTR and RLuc-EMCV IRES-FLuc-3' UTR were electroporated into siRNA-treated cells. After incubation for 1 day, Fluc and Rluc activities in the cell lysates were measured. For treatment with La inhibitor, the synthetic peptide derived from wild-type- (WT) or mutated (Y23Q) LA protein was pre-mixed with the above RNAs before the electroporation ($n = 3$). (C) HuH-7 derived cells replicating HCV SGR-JFH1/nanoluc RNA (SGR-GT2a) (genotype 2a, left panel) or SGR-Con1 RNA (SGR-GT1b) (genotype 1b, right panel) were transfected with siRNA and harvested at 72 h post-transfection. HCV RNA copies in the indicated cells were quantified ($n = 4$) (12-well plate). Expression of HCV NS5A and GAPDH in the indicated cells were examined by immunoblotting (lower) and protein levels were quantified by ImageJ. The intensity of each protein band for siRNA NC-transfected cells was set as 1, and the relative values were determined for siRPL17, siRNA YBX1, and siRNA PI4KA-transfected cells. (D) SGR-JFH1/nanoluc replicating cells were transfected with siRNA and harvested on day 2 and day 3 after siRNA transfection. Expression of NS3, NS5A, RPL17, YBX1, and GAPDH in the indicated cells was examined by immunoblotting, and protein levels were quantified by ImageJ. The intensity of each protein band for siRNA NC-transfected cells was set as 1, and the relative values were determined for siRNA RPL17, siRNA YBX1-transfected cells. (E) mRNA expression levels of genes indicated in HCVpp assay (A), IRES-dependent translation assay (B), and subgenomic replication assays (C) in siRNA-treated cells were determined by qRT-PCR. Results are presented as means \pm SD. Statistical analysis was conducted by ANOVA with post hoc Tukey's test for pairwise group comparisons. *** $P < 0.001$.

and that the presence or absence of the 3'X sequence in the replicons and knockdown of RPL17 or YBX1 had no effect on HCV RNA levels in the producer cells (Fig. 8D).

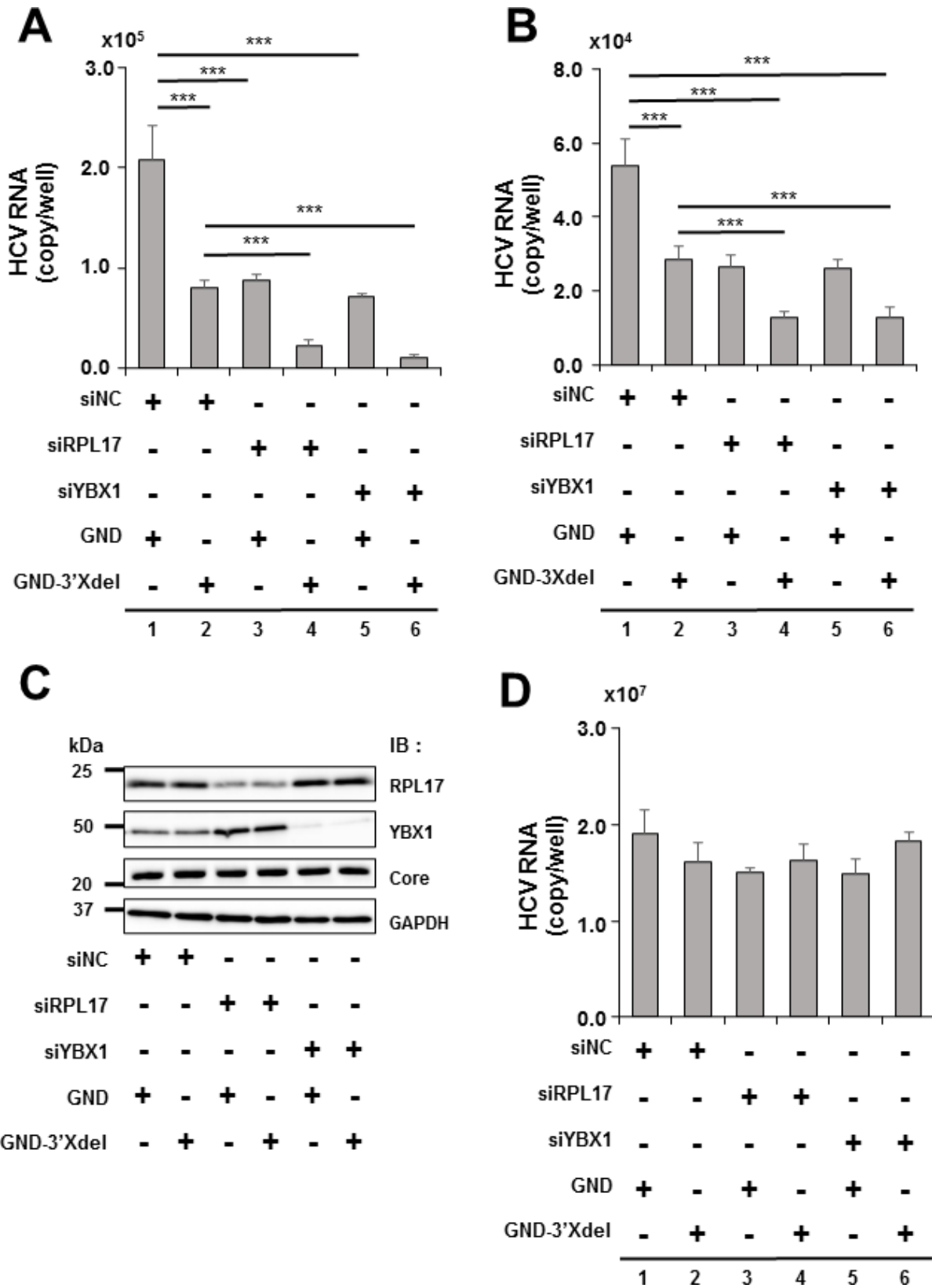


FIG 8 Particle production in the viral replication-defective setting was inhibited by the knocking down of RPL17 and YBX1. Huh7.5.1 cells expressing HCV Core-NS2 were transfected with siRNA and the viral SGR GND RNA or GND-3'Xdel RNA (producer cells). After culturing for 3 days, the culture supernatants collected were inoculated to naïve Huh7.5.1 cells (transducer cells), followed by measurement of HCV RNA copies at 3 dpi to determine the viral transduction (Continued on next page)

FIG 8 (Continued)

(A). Particle-associated HCV samples were prepared from the culture supernatants of the producer cells and the viral RNA copies were determined (B). Expression of RPL17, YBX1, HCV Core, and GAPDH (C) and the viral RNA copies (D) in the producer cells was determined by immunoblotting and qRT-PCR, respectively. The number of each sample group is indicated at the bottom of panels (A), (B), and (D). Results are presented as means \pm SD ($n = 4$). Statistical analysis was conducted by ANOVA with post hoc Tukey's test for pairwise group comparisons. *** $P < 0.001$.

Taken together, these results demonstrate that, while the expression of RPL17 and YBX1 has some influence on HCV RNA replication, both factors are most intensively involved in the particle formation process during the viral life cycle.

Possible involvement of RPL17 and YBX1 in HCV Core-RNA interaction

The association of HCV genomic RNA with Core protein is essential for the viral genome packaging and nucleocapsid formation. We thus hypothesized that RPL17 and YBX1 may contribute to nucleocapsid formation by promoting the Core-RNA interaction through their binding to the viral 3'UTR RNA. After the knockdown of cells in which HCV subgenomic RNA replicates and Core-NS2 is expressed by introducing siRNA against RPL17 or YBX1, cell lysates were immunoprecipitated with anti-Core antibody and HCV RNA levels in the precipitates were quantitatively measured. HCV RNA levels precipitated with the viral Core were significantly reduced in cells with knockdown of RPL17 or YBX1 (Fig. 9A). Knockdown of RPL17 or YBX1 had little effect on subgenomic RNA levels (Fig. 9B) or Core protein expression (Fig. 9C) in this experimental condition.

Microscopic observations of HCV-infected cells have shown that the viral Core protein is detected as co-localized with double-stranded (ds)RNA (22). Both RPL17 and YBX1 also colocalized with dsRNA in the cytoplasm of HCV-infected cells (Fig. 10). We thus analyzed the subcellular distribution of Core and dsRNA in HCV-infected cells using confocal microscopy with immunofluorescent antibodies and confirmed that both signals, which show dot-like shapes, co-localize mainly in the cytoplasmic region surrounding the nucleus of siRNA control cells (siNC) (Fig. 11A, upper). To quantitatively evaluate the co-localization of Core- and dsRNA signals, profiles of the distance in pixels were obtained from the fluorescence signal data (Fig. 11B). In the control cells, the pixel distance peak of the Core signal matched well with the peak of the dsRNA signal, confirming the co-localization of dsRNA and Core (Fig. 11B, upper). By contrast, when RPL17 or YBX1 was knocked down in HCV-infected cells, the pixel distance peaks of dsRNA and Core signals did not always coincide (Fig. 11B, middle and lower), indicating that the co-localization of Core and dsRNA was limited to a subset of molecules. Histograms of the frequency distribution of pixel distance showed that in RPL17- or YBX1 knockdown cells, there were not only fewer frequencies of Core-dsRNA co-localization (distance = 0), but also a greater number of signals with larger pixel distances (distance = 3 and 4) (Fig. 11C). The expression of RPL17 and YBX1 was sufficiently reduced by introduction with each siRNA, as confirmed by immunostaining (Fig. S4).

DISCUSSION

The initial process of particle formation of plus-stranded RNA viruses involves molecular mechanisms such as switching from genome replication to the process of capsid assembly, interaction with capsid proteins *via* packaging signals in the genome, and assembly into nucleocapsid. The 3'X region within the 3'UTR of the HCV genome has been reported not only to regulate translation and genome replication but to act as a cis-element for genome encapsidation. The 3'X plays a key role in controlling viral replication and translation by modulating the exposure of a nucleotide segment involved in a distal base-pairing interaction with an upstream 5BSL3.2 domain in the NS5B coding region. The IRES and the 3'X region are connected through domain 5BSL3.2, which establishes a network of distal RNA-RNA contacts involving both the IRES and domain 3'X. Several models have been proposed for the secondary structure of the

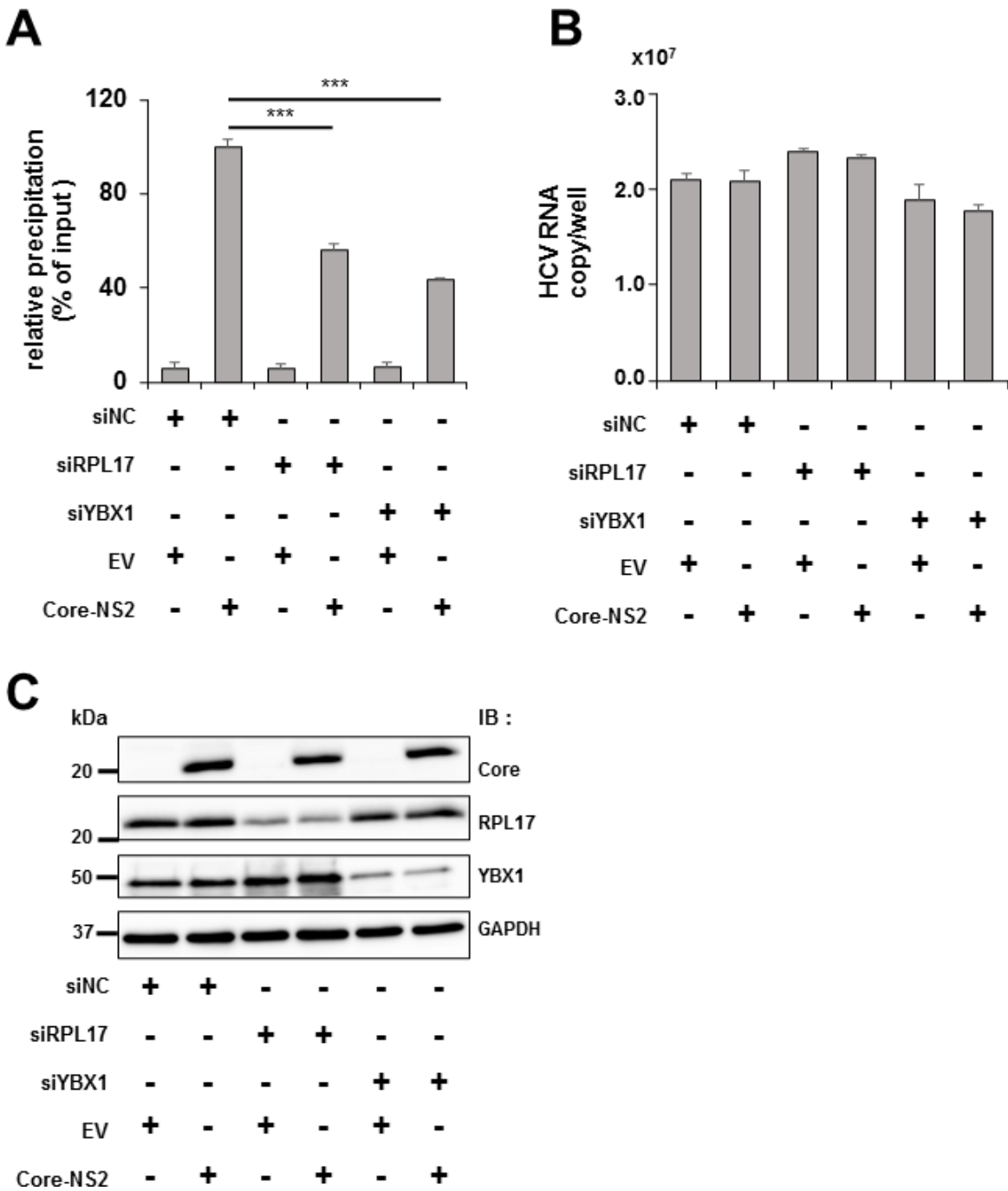


FIG 9 Interaction between HCV Core and the viral RNA was impaired by knocking down of RPL17 and YBX1. Cells replicating SGR-JFH1/NanoLuc were transfected with siRNA against RPL17 or YBX1 or negative control (NC) siRNA as well as the expression plasmid for Core-NS2 or pCAGGS (EV). After 2 days of culture, the protein-RNA complex was cross-linked by UV and immunoprecipitated by the anti-Core antibody. Amounts of immunoprecipitated HCV RNA were determined by qRT-PCR and ratios of immunoprecipitated HCV RNA copies to the input RNA copies were calculated. The ratio in the case of Core-NS2-expressing cells in the presence of siNC was set at 100 (A). Intracellular HCV RNA copies in the indicated cells (without immunoprecipitation) were quantified (B). Expression of RPL17, YBX1, HCV Core, and GAPDH in the indicated cells was examined by immunoblotting (C). Results are presented as means \pm SD ($n = 3$). Statistical analysis was conducted by ANOVA with post hoc Tukey's test for pairwise group comparisons. *** $P < 0.001$.

3'X, with the typical model being that it folds into two types of conformation: a three stem-loop conformation and a two stem-loop conformation.

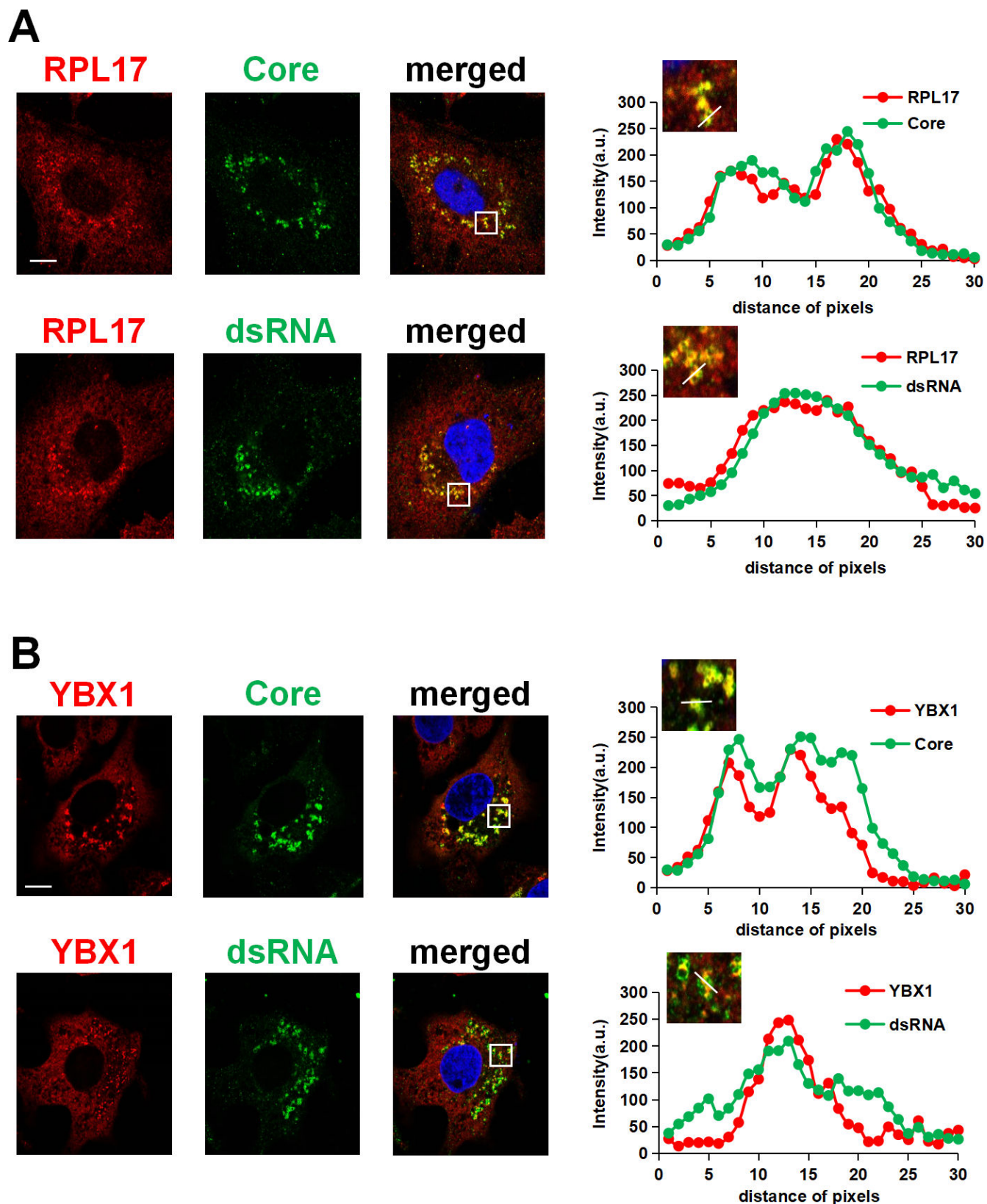


FIG 10 Co-localization of RPL17 and YBX1 with dsRNA and HCV Core in the viral infected cells. Expression of RPL17(A) and YBX1(B) in Huh7.5.1 cells infected with HCV J6/JFH-1 (MOI = 0.2) was examined by immunostaining with anti-RPL17 and anti-YBX1 antibodies, respectively (red). Anti-Core and anti-dsRNA antibodies (green) were used for the detection of HCV Core and dsRNA, respectively. DAPI (blue) was used as a nuclear counterstain. Intensity peaks of RPL17 and Core, (Continued on next page)

FIG 10 (Continued)

RPL17 and dsRNA, YBX1 and Core, and YBX1 and dsRNA were determined by line-scan analysis. The pixel distances of RPL17 and Core, RPL17 and dsRNA, YBX1 and Core, YBX1 and dsRNA (0.11 $\mu\text{m}/\text{pixel}$) were determined in line profile plots as shown on the right side of the micrographs. Representative line profile plots show the intensity distribution of green and red channels through the white lines indicated in the magnified views in merged panels. Bars indicate 10 μm .

In both conformations, the 3-terminal SLI is retained, but the upstream 55 nt long segment forms either one stem-loop such that the palindromic dimer linkage sequence (DLS) is exposed, or two stem-loops (SLII and SLIII) in which the DLS is not fully exposed (23–26). HCV RNA dimerization has been shown to regulate viral replication and translation processes; RNA interaction in the 3'X and 5BSL3.2 regions is important for genome replication, but DLS-DLS dimer formation interferes with this interaction, leading to suppression of replication. As the number of genomic RNA copies packaged into virions is limited, DLS-mediated dimerization may be involved in the switch from replication to particle formation, but it is unclear whether RNA conformational changes actually contribute to the switch from replication to particle formation. Host factors may also be involved in the regulation of such molecular switching and selective genome packaging, but this has not been investigated to date.

In this study, RNA-IP and LC-MS/MS analyses were combined to search for host factors that bind to HCV 3'UTR sequences in cells. In a proteomics screening for RNA-binding proteins, RPL17 and YBX1 showed dramatically reduced binding to SGR 3'Xdel RNA compared to SGR full-length RNA (Table 1), and *in vitro* binding analysis by AlphaScreen showed both proteins significantly reduced RNA binding with the 3'X deletion (Fig. 5A). Therefore, we hypothesize that the 3'X region is critical for HCV RNA binding by RPL17 and YBX1. However, the *trans*-packaging assay showed that even GND-3'Xdel RNA can be packaged to some extent, although its efficiency is markedly lower than that of SGR-GND RNAs, and the packaging efficiency was further reduced by the knockdown of RPL17 or YBX1 (Fig. 8A). These results suggest that while RPL17 and YBX1 function in particle formation potentially through binding to the 3'X region, both proteins may also contribute to the particle formation through their binding to the viral RNA region(s) other than 3'X. Indeed, AlphaScreen analysis shows that RPL17 and YBX1 remain binding to the SGR 3'Xdel (Fig. 5A). Mutational analysis of putative SLII within 3'X revealed that the binding capacities of RPL17 and YBX1 are greatly reduced in a mutant with a smaller loop structure (3'X/SL2mt3) and in a mutant that retains the loop structure but with sequence substitutions including DLS (3'X/SL2mt4)(Fig. 5C). Since 3'X within the 3'UTR of HCV genome can act as a packaging signal, one may hypothesize that binding of RPL17 and YBX1 to 3'X possibly contributes to encapsidation of the HCV genome. We thus addressed the possibility that RPL17 and YBX1 may have some influence on the association between HCV RNA and Core, as assessed by RNA-IP assay for the viral RNA-Core interaction in cells and by confocal microscopic imaging for intracellular co-localization. Knockdown of RPL17 or YBX1 resulted in reducing the amount of HCV RNA co-precipitating with Core to less than 50% (Fig. 9A) and in increasing the relative spatial distance between Core and dsRNA by imaging analysis (Fig. 11). These results suggest that expression of RPL17 and YBX1 potentially affects the interaction between HCV Core and viral RNA, leading to efficient encapsidation in the infected cells.

YBX1, which has a cold shock domain with broad nucleic acid binding properties, functions as a DNA- and RNA-binding protein and is involved in many cellular processes, including transcriptional and translational regulation, pre-mRNA splicing, DNA repair, and mRNA packaging (27–33). Systematic analysis of the RNA recognition specificities of RNA-binding proteins has demonstrated that YBX1 prefers sequences with complex combinations of G, C, and U (34). A sequence: CUGUC (underlined are consensus residues) similar to RNA motifs proposed as RNA-binding sequences by YBX1 is well conserved in the SLII domain within 3'X of 3'UTR among the HCV genome sequences derived from all genotypes. RPL17 is a component of the 60S subunit and belongs to the L6P family of ribosomal proteins (RPs); RPs function to facilitate intracellular translation processes and the correct folding of rRNA. Recently, in addition to their

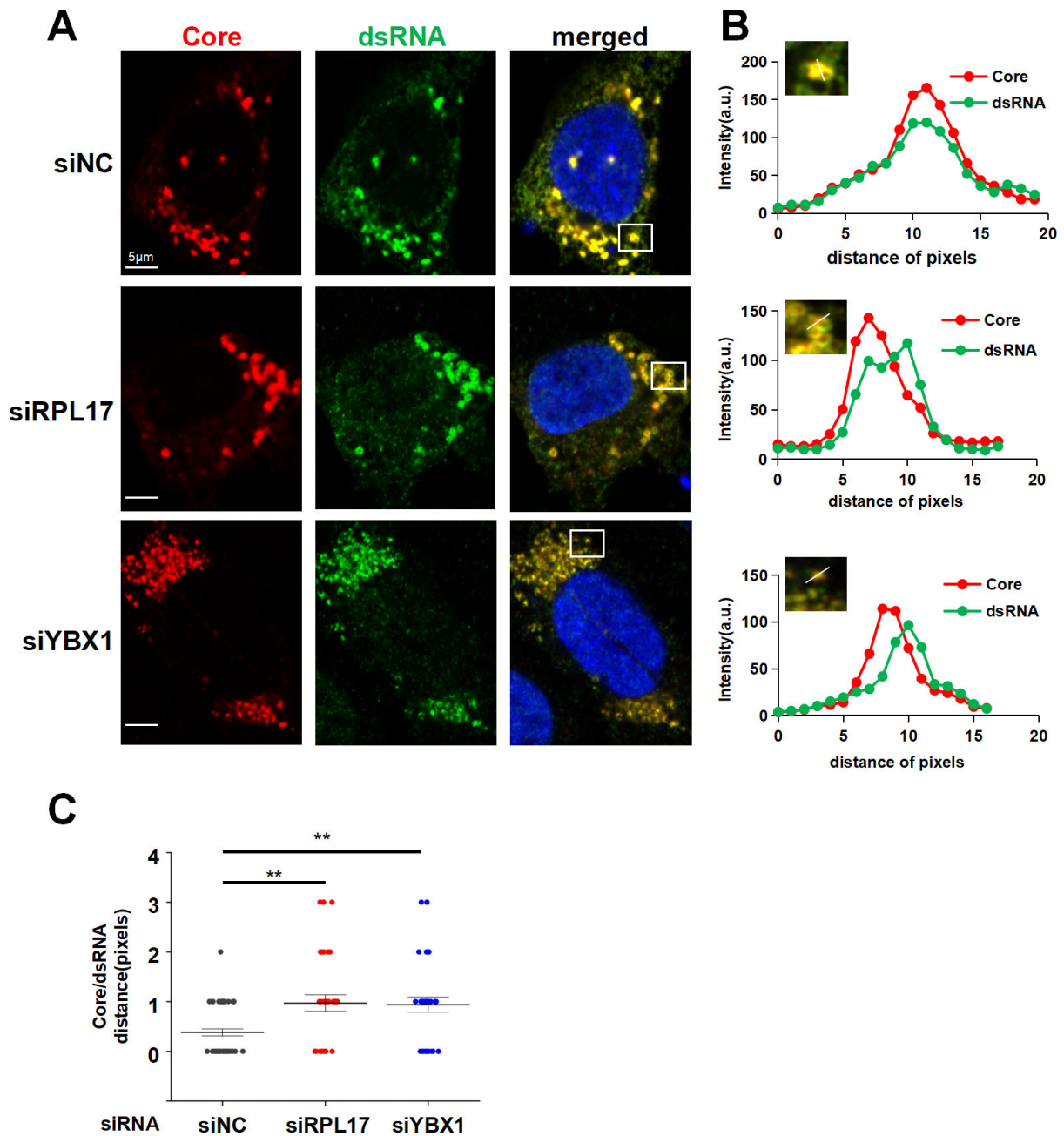


FIG 11 Effect of knocking down of RPL17 and YBX1 on colocalization of HCV Core and double-stranded (ds)RNA in the viral infected cells. Huh7.5.1 cells were transfected with siRNA against RPL17 or YBX1 negative control (NC) siRNA and infected with HCV J6/JFH-1 (MOI = 0.2). (A) Expression of HCV Core and dsRNA was examined by immunostaining with anti-Core- (red), anti-dsRNA (green) antibodies, and DAPI (blue). Bars indicate 5 μ m. (B) Intensity peaks of HCV Core and dsRNA were determined by line-scan analysis. Representative line profile plots show the intensity distribution of green and red channels through the white lines indicated in the magnified views in merged panels. (C) Frequency distribution histograms of HCV Core-dsRNA distance. The distances of Core and dsRNA in pixels (0.11 μ m/pixel) were determined in line profile plots as shown in (B). For the siNC (dark gray), siRPL17 (red) and siYBX1 (blue) groups, 55, 33, and 33 line profiles, respectively, were analyzed. Mean and SD values were also indicated.

involvement in protein synthesis, RPs have been shown to perform non-ribosomal functions such as transcriptional regulation, DNA repair, RNA splicing, cell proliferation, apoptosis regulation, and development (35–38). YBX1 has been shown to exhibit structural plasticity that unfolds structured mRNA into elongated linear filaments, possibly contributing to mRNA scanning by ribosomes during the initiation of mRNA translation and the elongation phase (33). NMR spectroscopy and molecular dynamics

analyses have revealed that YBX1 has ATP-independent unwinding activity of bound mRNA secondary structures *via* a loop structure, which is long and positively charged, within its cold shock domain (39). For RPL17, it is currently unclear whether binding to RNA leads to changes in the RNA secondary structure, but such a possibility is plausible given its function as indicated above. A working hypothesis is that binding of RPL17 and/or YBX1 to the 3'X region of the newly synthesized HCV genome alters the RNA secondary structure, such as unwinding, which may facilitate Core-RNA binding. In HCV-infected cells, simultaneous knockdown of the RPL17 and YBX1 genes showed a similar degree of inhibition of particle production as knockdown of either RPL17 or YBX1 (Fig. 4A). We thus speculate that RPL17 and YBX1 play similar roles in the particle formation process and that the presence of both factors may result in an RNA structure suitable for genome packaging or nucleocapsid formation. To better understand the mechanisms of action of RPL17 and YBX1 in regulating HCV particle formation, our research is underway to prepare purified proteins of RPL17, YBX1, and Core for structural analysis of their complexes with HCV 3'X RNA. In the course of this research, it will be determined whether and how the secondary structure or conformation of the RNA is altered by the binding of RPL17 or YBX1. It is also planned to determine whether the efficiency of association with Core actually differs between RPL17- or YBX1-bound 3'X RNA and unbound RNA.

It has been reported on the involvement of YBX1 in the HCV life cycle. Chatel-Chaix et al. have identified YBX1 as an interacting partner of NS3/4A and shown that the knockdown of YBX1 stimulated the release and/or egress of HCV particles without affecting virus assembly (40, 41). Wang et al. have revealed that YBX1 may modulate various steps of the HCV life cycle including particle production *via* maintaining NS5A level in cells (42). The effect of YBX1 knockdown on RNA replication varied depending on the experimental systems and conditions. In particle formation, one group has shown that YBX1 knockdown led to enhancing the viral particle production, while the other group has reported the opposite: it suppressed virus production. In our subgenomic replication system, YBX1 knockdown resulted in a suppression of RNA levels of around 20%, which is moderate compared to the inhibitory effect on virus production. Although a previous study has reported YBX1 as an HCV 3'UTR binding factor (43) and another study has described RPL17 in the list of host factors that interact with NS3/4A (40), neither study has analyzed how the interaction is involved in the HCV life cycle. Since YBX1 and RPL17 can interact with NS3/4A and NS5A, which are involved in particle formation as well as replication, it may be likely that YBX1 and RPL17 are potentially involved in the switch from replication to capsid assembly in addition to genome packaging during particle formation. In this study, the knockdown of RPL17 in subgenomic replicon assays resulted in moderately but significantly increasing HCV RNA levels (Fig. 7C), suggesting that RPL17 expression may act in an inhibitory manner on RNA replication and thus may contribute to the transition from replication process to particle formation. While much has been learned about the host factors that interact with plus-stranded RNA viruses and are important in regulating their viral life cycles, to our knowledge, little is known about the host factors that bind to the RNA cis-elements important for genome encapsidation and are involved in the control of particle formation for their virus species. Although packaging signals have been identified for togaviruses such as alphaviruses, host factors involved in encapsidation have not been characterized. For flaviviruses, RNA-binding proteins involved in particle formation have been reported, including YBX1; knockdown of YBX1 in dengue virus- and Zika virus-infected cells has a limited effect on RNA replication, while particle production is significantly impaired (44–46). Although YBX1 has been reported to bind to the 3'UTR RNA of DENV, it is unclear whether YBX1 targets cis-elements involved in genome encapsidation (47).

In general, viral genomic RNAs are presumed to change conformation during the course of the viral infection cycle, but how they actually change inside the cell is largely unknown to date. In addition to *in vitro* structural analyses of the HCV 3'UTR

in the presence or absence of YBX1, RPL17, or Core, the application of recently developed methods, such as *in vivo* single-molecule RNA secondary structural profiling (48) and live-cell single-molecule imaging, VIRIM (Virus Infection Real-time IMaging) (49), to continuous analyses focusing on the process from replication to particle formation during HCV infection is likely to help elucidate the fine details of virus-host interaction patterns characteristic of the initiation of nucleocapsid formation, as well as RNA conformations important for this process.

MATERIALS AND METHODS

Antibodies

Mouse monoclonal antibody against HCV Core (2H9) was generated as described previously (6). Mouse monoclonal antibodies against GAPDH (6C5, Santa Cruz Biotechnology), RPL17 (67223-1-Ig, Proteintech for Immunoblotting; HPA046385, Sigma-Aldrich for immunofluorescence), full-length GFP (JL-8, Clontech), PI4KA (12411-1-AP, Proteintech), DYKDDDDK (012-22384, FUJIFILM Wako) and dsRNA (J2, Jena Bioscience) and rabbit polyclonal antibodies against YBX1 (ab76149, Abcam) and HCV NS3 (GTX131276, GeneTex) were used.

Plasmid construction

A replication-defective subgenomic replicon plasmid pSGR-JFH1 Δ 3'X/nanoluc-GND, which carries JFH-1-derived HCV sequence with NS5B mutation deleting 3'X region and nanoluc gene, was constructed from pSGR-JFH1/nanoluc-GND (50) by PCR site-directed mutagenesis with KOD FX neo (TOYOBO). To generate mutant plasmids with substitutions in 3'X region, double-stranded (ds)DNA fragments containing 3'X mutants (3'X/SL1mt, 3'X/SL2mt1, 3'X/SL2mt2, 3'X/SL2mt3, 3'X/SL2mt4) were synthesized by Integrated DNA Technologies (IDT) and inserted into pSGR-JFH1 Δ 3'X/nanoluc-GND. To construct expression plasmids for RPL17 and YBX1, dsDNA fragments of optimized sequence for RPL17 and YBX1 (IDT) were inserted into pCAG-neo (Wako) and pEU-E01 vector (CellFree Sciences). Synthesized FLAG sequence was further inserted into the 3' sites of RPL17 and YBX1 sequence in these plasmids by inverted PCR, resulting in pCAG-RPL17-FLAG, pCAG-YBX1-FLAG, pEU-RPL17-FLAG, and pEU-YBX1-FLAG. Expression plasmids with partial deletions in RPL17 and YBX1 regions were constructed from pEU-RPL17-FLAG and pEU-YBX1-FLAG by inverted PCR. To construct an expression plasmid for GFP-FLAG, a DNA fragment of super folder GFP gene which was prepared by PCR with pHRdSV40-scFv-GCN4-sfGFP-VP64-GB1-NLS (60904, Addgene) (51) as a template was inserted into pEU-E01, followed by inserting the FLAG sequence into the resulting plasmid (pEU-sfGFP). To construct IRES reporter plasmids containing HCV 3'UTR, a DNA fragment for HCV 3'UTR which was amplified from pSGR-JFH1/nanoluc-GND was inserted into pRL-HCV Luc and pRL-EMCV Luc (52), resulting in pRL-HCV Luc-3'UTR and pRL-EMCV Luc-3'UTR. To construct HCV Core-NS2 in phiC31 Integrase vector system (System Biosciences), a DNA fragment for Core-E1-E2-p7-NS2 region was amplified from pCAG-Core-NS2 (16) by PCR and inserted into pFC-CMV-MCS-pA-SV40-Neo, resulting in pFC-Core-NS2.

Cell culture and transfection

The human hepatoma cell line Huh-7, its derivative cell line Huh7.5.1 (a gift from Francis V. Chisari, The Scripps Research Institute), and the human embryonic kidney cell line 293T used to generate HCV pseudoparticles (HCVpp) were maintained in Dulbecco modified Eagle medium supplemented with nonessential amino acids, 100 U of penicillin/mL, 100 μ g of streptomycin/mL, and 10% fetal bovine serum. Huh5-15 cells, which carry the subgenomic HCV replicon derived from the Con1 strain (a gift from Ralf Bartenschlager, University of Heidelberg, Heidelberg, Germany), and SGR-JFH1/nanoluc cells, which harbor the subgenomic HCV replicon from JFH-1 strain and a

nanoluc luciferase reporter gene fused to the neomycin phosphotransferase gene of pSGR-JFH1, were cultured in the above medium supplemented with 0.2 mg/mL G418. Persistently HCV-infecting Huh-7 cells (HC-PI cells) were obtained by infected with cell culture-derived HCV of JFH-1 strain at a multiplicity of infection (MOI) of 0.01. Cells were maintained in the above medium by passaging every 3–4 days for approximately 6 months. To establish HCV Core-NS2 stably expressing cells line, pFC-Core-NS2 and phiC31 integrase expression plasmids (System Biosciences) were co-transfected with Lipofectamine LTX with Plus reagent (Life Technologies) into Huh7.5.1 cells, followed by selection with 1 µg/mL puromycin for 7 days. For HCV RNA transfection, *in vitro* transcribed HCV RNAs were transfected into cells using TransIT-mRNA Transfection Reagent (Thermo Fisher Scientific). For gene silencing, siRNAs for RPL17 (s12179), YBX1 (s224139), CD81 (s2722), ApoE (s536402), PI4KAP2 (s200608), which were purchased from Ambion (Life Technologies), were transfected into cells using Lipofectamine RNAiMAX Transfection reagent (Life Technologies).

Virus stock and infection

HCV stocks were prepared as described previously (53, 54). For focus-forming unit (FFU) assay to determine the virus infectivity, Huh7.5.1 cells infected with diluted HCV samples for 72 h were fixed with cold methanol for 15 min and dried up for 30 min. The cells were then permeabilized with 0.3% Triton X-100 containing blocking solution (Block Ace, Yukijirushi) for 1 h and incubated with the anti-HCV Core antibody for 2 h and goat anti-mouse IgG-Alexa488 (Life Technologies) for 1 h at room temperature. The number of fluorescent cells was analyzed by IN Cell Analyzer 2200 (Cytiva). HCVpp was generated as described previously (52). Culture supernatants containing HCVpp were collected at 36 h and 60 h, respectively, after plasmid transfection and stored at –80°C before use. To assess virus entry activity into cells, an aliquot of HCVpp was inoculated into Huh7.5.1 cells and incubated for 2 days, followed by determination of Nanoluc activity in the cell lysates.

RNA extraction and quantitative (q)RT-PCR

To quantify cellular gene expression, total RNAs from cultured cells were isolated by TRI reagent (Molecular Research Center) and reverse-transcribed using the SuperScript VILO cDNA Synthesis Kit (Life Technologies). Aliquots of cDNAs were subjected to 45 cycles of PCR amplification. qRT-PCR was performed in the CFX Connect Real-Time System (Bio-Rad) using the THUNDERBIRD Next SYBR qPCR mix (TOYOBO). Relative RNA expression data were normalized to that of GAPDH mRNA using the comparative threshold method ($\Delta\Delta CT$). To determine HCV RNA copies in cells, total RNAs isolated from cells were checked concentration by Nanodrop (Thermo Fisher Scientific), then diluted RNAs to 0.01 µg/µL, and aliquots of RNAs were subjected to RT-PCR amplification. For particle-associated HCV RNA, culture supernatants were collected from infected cells and treated with PNE solution (8.45% PEG, 0.445 M NaCl, 13 mM EDTA) for 1 h on ice. To remove free nucleic acids, pellets were incubated for 1 h at 37°C with RNase A (Invitrogen). After treatment with proteinase K (Nacalai Tesque) at 56°C overnight, RNA was isolated by phenol/chloroform extraction and ethanol precipitation. qRT-PCR was performed in the CFX Connect Real-Time System using TaqMan Fast Virus 1-Step Master Mix (Applied Biosystems). The sequences of PCR primers used are listed in Table 2.

RNA synthesis and electroporation

RNA synthesis was performed as previously described (52). Briefly, linearized DNAs as templates were prepared by digesting with *Xba*I for pUC19, *Not*I for pBluescript backbone, and *Eco*RV for pRL-CMV backbone, respectively. RNAs were synthesized *in vitro* by a MEGascript T7 kit (Invitrogen) and treated with DNase I followed by acid phenol extraction. For electroporation, trypsinized cells were washed with PBS and resuspended at 1×10^5 cells/10 µL with BTXpress buffer (BTX). One microgram of

TABLE 2 Primer sets for qRT-PCR

Primer name	Orientation	Primer sequence
HCV qPCR	Forward	5'-GAGTGTGTCGTCAGCCTCCA-3'
	Reverse	5'-CACTCGCAAGCACCTATCA-3'
RPL17 qPCR	Forward	5'-GATTGTTCCCTAAACCAGAAGAGGA-3'
	Reverse	5'-TGAATTTACTCCCGTGCCATA-3'
YBX1 qPCR	Forward	5'-CCACAGTATTCCAACCCTCCT-3'
	Reverse	5'-CTGCCTCACTGGTCTACCTTG-3'
ApoE qPCR	Forward	5'-AAGGTGGAGCAAGCGGTGGAGAC-3'
	Reverse	5'-TGCACCCAGCGCAGGTAATC-3'
PI4KA qPCR	Forward	5'-GTGTCGCACTCATCAACAAGCTGG-3'
	Reverse	5'-CACACTGCATCATCCAGATTTGTC-3'
CD81 qPCR	Forward	5'-TCGTCTCAATTCGTCTTCTG-3'
	Reverse	5'-CTCCCAGCTCCAGATACAGG-3'
GAPDH qPCR	Forward	5'-AACAGCTCAAGATCATCAGC-3'
	Reverse	5'-GGATGATGTTCTGGAGAGCC-3'

reporter replicon RNA was mixed with 10 μ L of cell suspension and electroporated by Neon (Thermo Fisher Scientific). The condition of electroporation was at 1,400 V, 20 ms, and 1 pulse.

HCV IRES activity assay

Bicistronic reporter RNAs were *in vitro* transcribed from linearized pRL-HCV Luc-3'UTR and pRL-EMCV Luc-3'UTR by MEGAscript T7 kit (Invitrogen). The RNAs were incubated with or without La-derived peptide (WT LAP and Y23Q LAP were synthesized by Eurofins Genomics for 1 h at 37°C as previously described (55), followed by electroporation into siRNA-treated cells. The electroporated cells were lysed with 150 μ L passive lysis buffer (Promega) and Fluc and Rluc activity were measured by GloMax Discover (Promega) with ONE-Glo Luciferase Assay system (Promega) and Renilla-Glo Luciferase Assay System (Promega), respectively.

Immunoblotting

Immunoblotting was performed as previously described with slight modification (56). Briefly, cell lysates were separated by SDS-PAGE and transferred onto polyvinylidene difluoride membranes. After blocking, membranes were incubated with a primary antibody overnight at 4°C. After washing, membranes were incubated with an HRP-conjugated secondary antibody (Cell Signaling Technology) for 1 h. Chemiluminescence was detected using the FUSION (Vilber Bio Imaging). The intensity of the protein bands was measured by the Fiji version of ImageJ software (<https://imagej.net/software/fiji/downloads>), and the band intensity of the target protein with gene knockdown was calculated relative to that of the negative control.

Immunofluorescence

For indirect immunofluorescence, cells grown on a glass bottom plate were fixed with 4% paraformaldehyde in PBS for 30 min at room temperature. Cells were permeabilized in 0.5% Triton X-100 in PBS for 10 min at room temperature, followed by blocking with 1% bovine serum albumin. Immunocytochemistry was performed with a primary antibody, followed by incubation with Alexa Fluor 488 goat anti-mouse IgG and Alexa Fluor 555 goat anti-rabbit IgG for 1 h at room temperature. In experiments where HCV Core and dsRNA were detected simultaneously, the anti-Core antibody was fluorescently labeled in advance with Mix-n-Stain CF555 Antibody Labeling Kit (Biotium). dsDNA was stained with DAPI (Sigma-Aldrich). Confocal images were acquired with Confocal Laser Microscope AXR/Super-Resolution Microscope N-SIM S (Nikon). Intensity peaks of HCV

Core and dsRNA were examined by line-scan analysis on representative HCV-infected cells. The distance of pixels for HCV Core and dsRNA was analyzed by the ImageJ software.

Wheat germ cell-free protein synthesis

RNAs with FLAG sequence for full-length- or partially deleted RPL17 and YBX1 as well as for GFP were *in vitro* transcribed from pEU-RPL17-FLAG, pEU-RPL17-delN-FLAG, pEU-RPL17-delIM-FLAG, pEU-RPL17-delC-FLAG, pEU-YBX1-FLAG, pEU-YBX1-delCSD-FLAG, and pEU-GFP-FLAG, respectively. *In vitro* transcription was conducted in the presence of SP6 RNA polymerase for 6-h incubation in 37°C as described (57). The synthesized RNAs were subjected to cell-free protein synthesis using the WEPRO 1240 Expression kit (CellFree Sciences) by incubating for 16 h at 26°C according to the manufacturer's instruction.

RNA-immunoprecipitation (RIP) assay

After 24 h of siRNA transfection, SGR-JFH1/nanoluc cells were transfected with pCAGGS-Core-NS2 or pCAGGS empty vector. After 48 h of plasmids transfection, the cells were cross-linked by UV crosslinker and lysed by lysis buffer (RN1001, MBL). One-tenth volume of the cell lysates was transferred into new tubes and used as input samples. Core-RNA complexes were immunoprecipitated with anti-Core antibody-immobilized beads and the tubes were rotated overnight at 4°C, followed by separating the beads from the supernatants using a magnetic stand and washed three times with wash buffer (RN1001, MBL). RNAs associated with the beads were then isolated with TRI reagent.

Identification of host proteins binding to HCV 3'X RNA

RNAs prepared by *in vitro* transcription were electroporated into HCV Core-NS2 expressing Huh7.5.1 cells seeded into 10 cm dishes. Each replicon RNA (200 µg) prepared by *in vitro* transcription, as described above, was mixed with a suspension of Huh7.5.1 cells expressing HCV Core-NS2 (2×10^7 cells/2 mL), followed by electroporation using Neon (Thermo Fisher Scientific). After 24-h incubation, the cells were washed and cross-linked by UV crosslinker (UVP, HL-2000 HybriLinker, 0.15 J/cm²) on ice, immediately followed by scraping the cells and pelleting down by centrifugation at $1,500 \times g$ for 5 min. Cross-linked RNA-protein complexes were isolated essentially according to the procedure as described (58). The washed cell pellets were re-suspended in 600 µL of PBS, mixed with 200 µL of each: neutral phenol, toluol, and 1,3-bromochloropropane (BCP) at 2,000 rpm for 1 min (ThermoMixer, Eppendorf) and then centrifuged at $20,000 \times g$ for 3 min at 4°C. After removing the upper aqueous phase, 600 µL neutral phenol and 200 µL BCP were added, mixed, and centrifuged at $20,000 \times g$ for 3 min at 4°C. After phase separation, the three-fourth of the upper phase and the three-fourth of the lower phase were removed from the tube. The resulting interphase was mixed with 400 µL water, 200 µL ethanol, 400 µL neutral phenol, and 200 µL BCP at 2,000 rpm for 1 min as above and centrifuged at $20,000 \times g$ for 3 min at 4°C. After removing the upper and lower phases, the resulting interphase was mixed with 9 volumes of ethanol and kept at -20°C overnight, and centrifuged at $20,000 \times g$ for 30 min to precipitate the RNA-protein complex. The precipitates dried were dissolved with 100 µL nuclear-free water and incubated for 5 min at 56°C, followed by centrifugation at $2,000 \times g$ for 2 min. The supernatant samples were subjected to affinity purification of RNA-binding proteins, as described (59). Mixtures of the above samples with equal volumes of 2× affinity purification buffer and biotinylated oligonucleotide (5'-TCAGGTGTCTCCCTCCCTTG-3'; 10 pM at final concentration) were incubated at 70°C for 10 min and slowly cooled down to 49°C for oligonucleotide annealing with HCV RNA. NanoLink streptavidin magnetic beads (Vector Laboratories) were added to the resulting samples and rotated at 4°C overnight, followed by separating the beads from the supernatant using a magnetic stand. The beads were then washed sequentially with four kinds of wash buffers (Wash

Buffer 1: 20 mM Tris-HCl pH 7.5, 500 mM LiCl, 0.5% LiDS, 1 mM EDTA, 5 mM DTT; Wash Buffer 2: 20 mM Tris-HCl pH 7.5, 500 mM LiCl, 0.1% LiDS, 1 mM EDTA, 5 mM DTT; Wash Buffer 3: 20 mM Tris-HCl pH 7.5, 500 mM LiCl, 1 mM EDTA, 5 mM DTT; Wash Buffer 4: 20 mM Tris-HCl pH 7.5, 200 mM LiCl, 1 mM EDTA, 5 mM DTT). The resulting beads were treated with RNase A solution [20 μ L/mL RNase A and T1 cocktail (Life Technologies)], 20 mM Tris-HCl pH 7.5, 1 mM EDTA, 150 mM NaCl, 0.5 mM DTT) for 60 min at 37°C to digest the HCV RNAs bound to the beads. The supernatants containing proteins were separated from the beads using a magnetic stand and subjected to protein identification.

Proteins were identified by MS/MS analysis as follows. In brief, 500 μ L cold acetone was added to the sample tube containing proteins and was stored at -20°C overnight. After centrifugation at 12,000 rpm for 10 min, the pellet was dried up for 5 min at room temperature and dissolved with 100 μ L sampling buffer (25 mM ammonium bicarbonate with ultrapure water) and 50 μ L reducing agent (sampling buffer containing 10 mM DTT). The mixture was then incubated for 45 min at 56°C, added with 50 μ L alkylating agent (sampling buffer containing 10 mg/mL Iodoacetamide), and incubated for 30 min in a dark place. For preparation of tryptic peptides, the resulting solution was incubated with 10 μ L of 0.1 μ g/ μ L TPCK-treated trypsin (Sigma-Aldrich) at 37°C overnight, followed by adding 0.5 μ L TFA (trifluoroacetic acid) and concentrating to 30–50 μ L by evaporation. The peptides in the solution diluted with 1 mL of 0.1% formic acid were purified by SepPAK (Waters) and concentrated to 30–50 μ L by evaporation. The resulting peptide solution was diluted with an appropriate volume of 0.1% formic acid and analyzed by Q Exactive Hybrid Quadrupole-Orbitrap Mass Spectrometer (Thermo Fisher Scientific) with Xcalibur (version 4.1.50).

Amplified luminescent proximity homogeneous assay (AlphaScreen)

Biotinylated RNAs were synthesized by MEGAscript T7 kit. The size and quality of RNA fragments were evaluated by 2% formaldehyde-agarose gel. The 3' end of synthesized RNAs was labeled with biotin by Pierce RNA 3' End Biotinylation Kit (Thermo Fisher Scientific). The interaction between RNA and protein was evaluated by Alpha technology. In brief, 30 μ L reaction solution [0.1 nM of biotinylated RNAs, 10 nM of *in vitro* synthesized FLAG-tagged protein, 0.1% BSA, 40 U RNase inhibitor, 20 μ g/mL anti-FLAG M2 acceptor beads, 20 μ g/mL streptavidin donor beads, 3 μ L of 10 \times AlphaScreen assay buffer (PerkinElmer)] was incubated for 60 min at 25°C. AlphaScreen signals (photon counts at 630 nm/s) were detected on an EnSpire plate reader (PerkinElmer).

Statistical analysis

Values are expressed as means of triplicate experiments with the standard deviations (SD). In most analyses, statistical analysis was performed using ANOVA, followed by Tukey's HSD test for post hoc pairwise comparisons between groups. A significance level of $P < 0.05$ was employed to determine statistically significant differences.

Experimental data obtained are available upon request.

ACKNOWLEDGMENTS

We are grateful to T. Mochizuki for secretarial work and to M. Yamamoto for their technical assistance at Hamamatsu University School of Medicine. We also thank Dr. Wakita (National Institute of Infectious Diseases, Japan) for providing HCV JFH-1 clone and plasmid constructs containing JFH-1-derived cDNAs, Dr. Chisari for providing Huh7.5.1 cells, and Prof. Bartenschlager for providing Huh5-15 cells. Huh7.5.1 cells are the Original Research Materials from Apath, LLC. Microscopy experiments and LC-MS/MS analyses were supported by the Advanced Research Facilities & Services, Preeminent Medical Photonics Education & Research Center, Hamamatsu University School of Medicine.

This work was supported by the Japan Agency for Medical Research and Development (AMED) under Grant nos. JP24fk0210145h0001,

JP24fk0210110s0103, JP24fk0310506h0103, JP23fk0310507h0002, JP24fk0310507s0603, and JP24fk03010521h0103, and by Hamamatsu University School of Medicine (HUSM)-in-Aid. This work was also supported by the scholarship donation from Yakult Co., Ltd.

AUTHOR AFFILIATION

¹Department of Microbiology and Immunology, Hamamatsu University School of Medicine, Shizuoka, Japan

AUTHOR ORCID*s*

Tetsuro Suzuki  <http://orcid.org/0000-0002-3754-789X>

FUNDING

Funder	Grant(s)	Author(s)
Japan Agency for Medical Research and Development (AMED)	JP24fk0210145h0001	Tetsuro Suzuki
Japan Agency for Medical Research and Development (AMED)	JP24fk0210110s0103	Tetsuro Suzuki
Japan Agency for Medical Research and Development (AMED)	JP24fk0310506h0103	Tetsuro Suzuki
Japan Agency for Medical Research and Development (AMED)	JP24fk03010521h0103	Tetsuro Suzuki
Japan Agency for Medical Research and Development (AMED)	JP23fk0310507h0002	Masahiko Ito
Japan Agency for Medical Research and Development (AMED)	JP24fk0310507s0603	Masahiko Ito

AUTHOR CONTRIBUTIONS

Jie Liu, Investigation, Visualization, Writing – original draft | Masahiko Ito, Data curation, Formal analysis, Funding acquisition, Investigation, Methodology, Validation, Visualization, Writing – original draft | Liang Liu, Investigation, Visualization | Kenji Nakashima, Methodology, Supervision, Validation | Shinya Satoh, Methodology, Supervision, Validation | Alu Konno, Methodology, Supervision, Validation | Tetsuro Suzuki, Conceptualization, Data curation, Funding acquisition, Project administration, Resources, Supervision, Writing – review and editing

ADDITIONAL FILES

The following material is available [online](#).

Supplemental Material

Supplemental figures (JVI00522-24-s0001.pdf). Figures S1 to S4.

REFERENCES

- Romero-López C, Berzal-Herranz A. 2017. The 5BSL3.2 functional RNA domain connects distant regions in the hepatitis C virus genome. *Front Microbiol* 8:2093. <https://doi.org/10.3389/fmicb.2017.02093>
- Cantero-Camacho Á, Gallego J. 2018. An unexpected RNA distal interaction mode found in an essential region of the hepatitis C virus genome. *Nucleic Acids Res* 46:4200–4212. <https://doi.org/10.1093/nar/gky074>
- Fukasawa M. 2010. Cellular lipid droplets and hepatitis C virus life cycle. *Biol Pharm Bull* 33:355–359. <https://doi.org/10.1248/bpb.33.355>
- Boson B, Granio O, Bartenschlager R, Cosset FL. 2011. A concerted action of hepatitis C virus p7 and nonstructural protein 2 regulates core localization at the endoplasmic reticulum and virus assembly. *PLoS Pathog* 7:e1002144. <https://doi.org/10.1371/journal.ppat.1002144>
- Awadh AA. 2023. The role of cytosolic lipid droplets in hepatitis C virus replication, assembly, and release. *Biomed Res Int* 2023:5156601. <https://doi.org/10.1155/2023/5156601>
- Masaki T, Suzuki R, Murakami K, Aizaki H, Ishii K, Murayama A, Date T, Matsuura Y, Miyamura T, Wakita T, Suzuki T. 2008. Interaction of hepatitis C virus nonstructural protein 5A with core protein is critical for the production of infectious virus particles. *J Virol* 82:7964–7976. <https://doi.org/10.1128/JVI.00826-08>
- Eyre NS, Hampton-Smith RJ, Aloia AL, Eddes JS, Simpson KJ, Hoffmann P, Beard MR. 2016. Phosphorylation of NS5A serine-235 is essential to hepatitis C virus RNA replication and normal replication compartment formation. *Virology* 491:27–44. <https://doi.org/10.1016/j.virol.2016.01.018>

8. Masaki T, Matsunaga S, Takahashi H, Nakashima K, Kimura Y, Ito M, Matsuda M, Murayama A, Kato T, Hirano H, Endo Y, Lemon SM, Wakita T, Sawasaki T, Suzuki T. 2014. Involvement of hepatitis C virus NS5A hyperphosphorylation mediated by casein kinase I-alpha in infectious virus production. *J Virol* 88:7541–7555. <https://doi.org/10.1128/JVI.03170-13>
9. Lindenbach BD. 2013. Virion assembly and release. *Curr Top Microbiol Immunol* 369:199–218. https://doi.org/10.1007/978-3-642-27340-7_8
10. Zayas M, Long G, Madan V, Bartenschlager R. 2016. Coordination of hepatitis C virus assembly by distinct regulatory regions in nonstructural protein 5A. *PLoS Pathog* 12:e1005376. <https://doi.org/10.1371/journal.ppat.1005376>
11. Chameettachal A, Mustafa F, Rizvi TA. 2023. Understanding retroviral life cycle and its genomic RNA packaging. *J Mol Biol* 435:167924. <https://doi.org/10.1016/j.jmb.2022.167924>
12. Kim DY, Firth AE, Atasheva S, Frolova EI, Frolov I. 2011. Conservation of a packaging signal and the viral genome RNA packaging mechanism in alphavirus evolution. *J Virol* 85:8022–8036. <https://doi.org/10.1128/JVI.00644-11>
13. Comas-Garcia M. 2019. Packaging of genomic RNA in positive-sense single-stranded RNA viruses: a complex story. *Viruses* 11:253. <https://doi.org/10.3390/v11030253>
14. Friebe P, Bartenschlager R. 2009. Role of RNA structures in genome terminal sequences of the hepatitis C virus for replication and assembly. *J Virol* 83:11989–11995. <https://doi.org/10.1128/JVI.01508-09>
15. Rheault M, Cousineau SE, Fox DR, Abram QH, Sagan SM. 2023. Elucidating the distinct contributions of miR-122 in the HCV life cycle reveals insights into virion assembly. *Nucleic Acids Res* 51:2447–2463. <https://doi.org/10.1093/nar/gkad094>
16. Shi G, Ando T, Suzuki R, Matsuda M, Nakashima K, Ito M, Omatsu T, Oba M, Ochiai H, Kato T, Mizutani T, Sawasaki T, Wakita T, Suzuki T. 2016. Involvement of the 3' untranslated region in encapsidation of the hepatitis C virus. *PLoS Pathog* 12:e1005441. <https://doi.org/10.1371/journal.ppat.1005441>
17. Shi G, Suzuki T. 2018. Molecular basis of encapsidation of hepatitis C virus genome. *Front Microbiol* 9:396. <https://doi.org/10.3389/fmicb.2018.00396>
18. Chang KS, Jiang J, Cai Z, Luo G. 2007. Human apolipoprotein E is required for infectivity and production of hepatitis C virus in cell culture. *J Virol* 81:13783–13793. <https://doi.org/10.1128/JVI.01091-07>
19. Benga WJA, Krieger SE, Dimitrova M, Zeisel MB, Parnot M, Lupberger J, Hildt E, Luo G, McLauchlan J, Baumert TF, Schuster C. 2010. Apolipoprotein E interacts with hepatitis C virus nonstructural protein 5A and determines assembly of infectious particles. *Hepatology* 51:43–53. <https://doi.org/10.1002/hep.23278>
20. Lee JY, Acosta EG, Stoeck IK, Long G, Hiet MS, Mueller B, Fackler OT, Kallis S, Bartenschlager R. 2014. Apolipoprotein E likely contributes to a maturation step of infectious hepatitis C virus particles and interacts with viral envelope glycoproteins. *J Virol* 88:12422–12437. <https://doi.org/10.1128/JVI.01660-14>
21. Matsumoto K, Wolffe AP. 1998. Gene regulation by Y-box proteins: coupling control of transcription and translation. *Trends Cell Biol* 8:318–323. [https://doi.org/10.1016/s0962-8924\(98\)01300-2](https://doi.org/10.1016/s0962-8924(98)01300-2)
22. Targett-Adams P, Boulant S, McLauchlan J. 2008. Visualization of double-stranded RNA in cells supporting hepatitis C virus RNA replication. *J Virol* 82:2182–2195. <https://doi.org/10.1128/JVI.01565-07>
23. Ivanyi-Nagy R, Kanevsky I, Gabus C, Lavergne J-P, Fichoux D, Penin F, Fossé P, Darlix J-L. 2006. Analysis of hepatitis C virus RNA dimerization and core-RNA interactions. *Nucleic Acids Res* 34:2618–2633. <https://doi.org/10.1093/nar/gkl240>
24. Shetty S, Kim S, Shimakami T, Lemon SM, Mihailescu MR. 2010. Hepatitis C virus genomic RNA dimerization is mediated via a kissing complex intermediate. *RNA* 16:913–925. <https://doi.org/10.1261/rna.1960410>
25. Palau W, Masante C, Ventura M, Di Primo C. 2013. Direct evidence for RNA-RNA interactions at the 3' end of the hepatitis C virus genome using surface plasmon resonance. *RNA* 19:982–991. <https://doi.org/10.1261/rna.037606.112>
26. Romero-López C, Barroso-DelJesus A, García-Sacristán A, Briones C, Berzal-Herranz A. 2014. End-to-end crosstalk within the hepatitis C virus genome mediates the conformational switch of the 3'X-tail region. *Nucleic Acids Res* 42:567–582. <https://doi.org/10.1093/nar/gkt841>
27. Horwitz EM, Maloney KA, Ley TJ. 1994. A human protein containing a "cold shock" domain binds specifically to H-DNA upstream from the human gamma-globin genes. *J Biol Chem* 269:14130–14139. [https://doi.org/10.1016/S0021-9258\(17\)36764-9](https://doi.org/10.1016/S0021-9258(17)36764-9)
28. Chen CY, Gherzi R, Andersen JS, Gaietta G, Jürchott K, Royer HD, Mann M, Karin M. 2000. Nucleolin and YB-1 are required for JNK-mediated interleukin-2 mRNA stabilization during T-cell activation. *Genes Dev* 14:1236–1248.
29. Capowski EE, Esnault S, Bhattacharya S, Malter JS. 2001. Y box-binding factor promotes eosinophil survival by stabilizing granulocyte-macrophage colony-stimulating factor mRNA. *J Immunol* 167:5970–5976. <https://doi.org/10.4049/jimmunol.167.10.5970>
30. Gaudreault I, Guay D, Lebel M. 2004. YB-1 promotes strand separation *in vitro* of duplex DNA containing either mispaired bases or cisplatin modifications, exhibits endonucleolytic activities and binds several DNA repair proteins. *Nucleic Acids Res* 32:316–327. <https://doi.org/10.1093/nar/gkh170>
31. Chattopadhyay R, Das S, Maiti AK, Boldogh I, Xie J, Hazra TK, Kohno K, Mitra S, Bhakat KK. 2008. Regulatory role of human AP-endonuclease (APE1/Ref-1) in YB-1-mediated activation of the multidrug resistance gene MDR1. *Mol Cell Biol* 28:7066–7080. <https://doi.org/10.1128/MCB.00244-08>
32. Chen X, Li A, Sun BF, Yang Y, Han YN, Yuan X, Chen RX, Wei WS, Liu Y, Gao CC, Chen YS, Zhang M, Ma XD, Liu ZW, Luo JH, Lyu C, Wang HL, Ma J, Zhao YL, Zhou FJ, Huang Y, Xie D, Yang YG. 2019. 5-methylcytosine promotes pathogenesis of bladder cancer through stabilizing mRNAs. *Nat Cell Biol* 21:978–990. <https://doi.org/10.1038/s41556-019-0361-y>
33. Kretov DA, Clément M-J, Lambert G, Durand D, Lyabin DN, Bollot G, Bauvais C, Samsonova A, Budkina K, Maroun RC, Hamon L, Bouhss A, Lescop E, Toma F, Curmi PA, Maucuer A, Ovchinnikov LP, Pastré D. 2019. YB-1, an abundant core mRNA-binding protein, has the capacity to form an RNA nucleoprotein filament: a structural analysis. *Nucleic Acids Res* 47:3127–3141. <https://doi.org/10.1093/nar/gky1303>
34. Ray D, Kazan H, Chan ET, Peña Castillo L, Chaudhry S, Talukder S, Blencowe BJ, Morris Q, Hughes TR. 2009. Rapid and systematic analysis of the RNA recognition specificities of RNA-binding proteins. *Nat Biotechnol* 27:667–670. <https://doi.org/10.1038/nbt.1550>
35. Wang W, Nag S, Zhang X, Wang MH, Wang H, Zhou J, Zhang R. 2015. Ribosomal proteins and human diseases: pathogenesis, molecular mechanisms, and therapeutic implications. *Med Res Rev* 35:225–285. <https://doi.org/10.1002/med.21327>
36. Boulon S, Westman BJ, Hutten S, Boisvert FM, Lamond AI. 2010. The nucleolus under stress. *Mol Cell* 40:216–227. <https://doi.org/10.1016/j.molcel.2010.09.024>
37. Warner JR, McIntosh KB. 2009. How common are extraribosomal functions of ribosomal proteins? *Mol Cell* 34:3–11. <https://doi.org/10.1016/j.molcel.2009.03.006>
38. Lindström MS, Zhang Y. 2008. Ribosomal protein S9 is a novel B23/NPM-binding protein required for normal cell proliferation. *J Biol Chem* 283:15568–15576. <https://doi.org/10.1074/jbc.M801151200>
39. Budkina K, El Hage K, Clément M-J, Desforges B, Bouhss A, Joshi V, Maucuer A, Hamon L, Ovchinnikov LP, Lyabin DN, Pastré D. 2021. YB-1 unwinds mRNA secondary structures *in vitro* and negatively regulates stress granule assembly in HeLa cells. *Nucleic Acids Res* 49:10061–10081. <https://doi.org/10.1093/nar/gkab748>
40. Chatel-Chaix L, Melançon P, Racine M-È, Baril M, Lamarre D. 2011. Y-box-binding protein 1 interacts with hepatitis C virus NS3/4A and influences the equilibrium between viral RNA replication and infectious particle production. *J Virol* 85:11022–11037. <https://doi.org/10.1128/JVI.00719-11>
41. Chatel-Chaix L, Germain M-A, Motorina A, Bonnel É, Thibault P, Baril M, Lamarre D. 2013. A host YB-1 ribonucleoprotein complex is hijacked by hepatitis C virus for the control of NS3-dependent particle production. *J Virol* 87:11704–11720. <https://doi.org/10.1128/JVI.01474-13>
42. Wang WT, Tsai TY, Chao CH, Lai BY, Wu Lee YH. 2015. Y-box binding protein 1 stabilizes hepatitis C virus NS5A via phosphorylation-mediated interaction with NS5A to regulate viral propagation. *J Virol* 89:11584–11602. <https://doi.org/10.1128/JVI.01513-15>
43. Harris D, Zhang Z, Chaubey B, Pandey VN. 2006. Identification of cellular factors associated with the 3'-nontranslated region of the hepatitis C

- virus genome. *Mol Cell Proteomics* 5:1006–1018. <https://doi.org/10.1074/mcp.M500429-MCP200>
44. Diosa-Toro M, Kennedy DR, Chuo V, Popov VL, Pompon J, Garcia-Blanco MA. 2022. Y-box binding protein 1 interacts with dengue virus nucleocapsid and mediates viral assembly. *mBio* 13:e0019622. <https://doi.org/10.1128/mbio.00196-22>
45. Bonenfant G, Williams N, Netzband R, Schwarz MC, Evans MJ, Pager CT. 2019. Zika virus subverts stress granules to promote and restrict viral gene expression. *J Virol* 93:e00520-19. <https://doi.org/10.1128/JVI.00520-19>
46. Phillips SL, Soderblom EJ, Bradrick SS, Garcia-Blanco MA. 2016. Identification of proteins bound to dengue viral RNA *in vivo* reveals new host proteins important for virus replication. *mBio* 7:e01865-15. <https://doi.org/10.1128/mBio.01865-15>
47. Paranjape SM, Harris E. 2007. Y box-binding protein-1 binds to the dengue virus 3'-untranslated region and mediates antiviral effects. *J Biol Chem* 282:30497–30508. <https://doi.org/10.1074/jbc.M705755200>
48. Yang M, Zhu P, Cheema J, Bloomer R, Mikulski P, Liu Q, Zhang Y, Dean C, Ding Y. 2022. *In vivo* single-molecule analysis reveals *COOLAIR* RNA structural diversity. *Nature* 609:394–399. <https://doi.org/10.1038/s41586-022-05135-9>
49. Bruurs LJM, Müller M, Schipper JG, Rabouw HH, Boersma S, van Kuppeveld FJM, Tanenbaum ME. 2023. Antiviral responses are shaped by heterogeneity in viral replication dynamics. *Nat Microbiol* 8:2115–2129. <https://doi.org/10.1038/s41564-023-01501-z>
50. Kato T, Date T, Miyamoto M, Sugiyama M, Tanaka Y, Orito E, Ohno T, Sugihara K, Hasegawa I, Fujiwara K, Ito K, Ozasa A, Mizokami M, Wakita T. 2005. Detection of anti-hepatitis C virus effects of interferon and ribavirin by a sensitive replicon system. *J Clin Microbiol* 43:5679–5684. <https://doi.org/10.1128/JCM.43.11.5679-5684.2005>
51. Tanenbaum ME, Gilbert LA, Qi LS, Weissman JS, Vale RD. 2014. A protein-tagging system for signal amplification in gene expression and fluorescence imaging. *Cell* 159:635–646. <https://doi.org/10.1016/j.cell.2014.09.039>
52. Ito M, Sun S, Fukuhara T, Suzuki R, Tamai M, Yamauchi T, Nakashima K, Tagawa YI, Okazaki S, Matsuura Y, Wakita T, Suzuki T. 2017. Development of hepatoma-derived, bidirectional oval-like cells as a model to study host interactions with hepatitis C virus during differentiation. *Oncotarget* 8:53899–53915. <https://doi.org/10.18632/oncotarget.19108>
53. Wakita T, Pietschmann T, Kato T, Date T, Miyamoto M, Zhao Z, Murthy K, Habermann A, Kräusslich H-G, Mizokami M, Bartenschlager R, Liang TJ. 2005. Production of infectious hepatitis C virus in tissue culture from a cloned viral genome. *Nat Med* 11:791–796. <https://doi.org/10.1038/nm1268>
54. Akazawa D, Date T, Morikawa K, Murayama A, Miyamoto M, Kaga M, Barth H, Baumert TF, Dubuisson J, Wakita T. 2007. CD81 expression is important for the permissiveness of Huh7 cell clones for heterogeneous hepatitis C virus infection. *J Virol* 81:5036–5045. <https://doi.org/10.1128/JVI.01573-06>
55. Li X, Ito M, Aoyagi H, Murayama A, Aizaki H, Fukasawa M, Kato T, Wakita T, Suzuki T. 2022. Development and use of a kinetical and real-time monitoring system to analyze the replication of hepatitis C virus. *Int J Mol Sci* 23:8711. <https://doi.org/10.3390/ijms23158711>
56. Li Y, Ito M, Sun S, Chida T, Nakashima K, Suzuki T. 2016. LUC7L3/CROP inhibits replication of hepatitis B virus via suppressing enhancer II/basal core promoter activity. *Sci Rep* 6:36741. <https://doi.org/10.1038/srep36741>
57. Sawasaki T, Seki M, Sinozaki K, Endo Y. 2002. High-throughput expression of proteins from cDNAs catalogue from Arabidopsis in wheat germ cell-free protein synthesis system. *Tanpakushitsu Kakusan Koso* 47:1003–1008.
58. Urdaneta EC, Vieira-Vieira CH, Hick T, Wessels HH, Figini D, Moschall R, Medenbach J, Ohler U, Granneman S, Selbach M, Beckmann BM. 2019. Purification of cross-linked RNA-protein complexes by phenol-toluol extraction. *Nat Commun* 10:990. <https://doi.org/10.1038/s41467-019-08942-3>
59. Phillips SL, Garcia-Blanco MA, Bradrick SS. 2015. Antisense-mediated affinity purification of dengue virus ribonucleoprotein complexes from infected cells. *Methods* 91:13–19. <https://doi.org/10.1016/j.jymeth.2015.08.008>